5-2007

Direct analysis of solid corrosion products by laser ablation ICP-MS: Method development and the interaction of aqueous uranium, gadolinium and neodymium with Iron Shot and Iron (III) Oxide

James Cizdziel

Klaus J. Stetzenbach
University of Nevada, Las Vegas, STETZENB@unlv.nevada.edu

Amy J. Smiecinski
University of Nevada, Las Vegas, smiecins@unlv.nevada.edu

Nevada System of Higher Education
Errata Sheet

Page: 1 of:

1 Report Number:	2. Title:	3. Task
TR-06-005	Direct Analysis of Solid Corrosion Products by Laser Ablation ICP-MS: Method Development and the Interaction of Aqueous Uranium, Gadolinium and Neodymium with Iron Shot and Iron (III) Oxide	UNLV Research Foundation Cooperative Agreement # DE-FC28-04RW12237 ORD-RF-03

4. The following errors, defects, or concerns have been identified with the above listed product.

A key dataset supporting this report, R03JC.003, was found to contain some errors. The calibration curve for R03JC.003, generated from NIST glass, was determined using the wrong units (ppb instead of ppm). This error is known to have affected section 7.2.5 and Tables 4 and 5 of the report. A review by the author determined that the errors have no impact on the report's conclusions. However, this review was informal and was not conducted in accordance with qualified review procedures.

It is therefore recommended that users of this report consult the originating organization, UNLV/HRC/Chemistry Division, before using results from this report for any quality affecting purposes.

5. TEDS	Date:
Raymond E. Keeler	04/17/2008

Nevada System of Higher Education

TECHNICAL REPORT

Direct Analysis of Solid Corrosion Products by Laser Ablation ICP-MS: Method Development and the Interaction of Aqueous Uranium, Gadolinium and Neodymium with Iron Shot and Iron (III) Oxide

Report Document Identifier:
TR-06-005, Rev. 0
Task: ORD-RF-03

Author:	**James Cizdziel**	[redacted]	5/22/07 Date
PI:	**Klaus Stetzenbach**	[redacted]	23 MAY 07 Date
QA Manager:	**Amy Smiecinski**	[redacted]	5-23-07 Date

1.0 TABLE OF CONTENTS

ABBREVIATIONS, ACRONYMS, AND SYMBOLS 3
ACKNOWLEDGMENTS 3
STUDY TEAM 3
LIST OF TABLES 4
LIST OF FIGURES 5
2.0 PURPOSE, SCOPE AND ORGANIZATION OF THE REPORT 7
2.1 Purpose 7
2.2 Scope 7
2.3 Organization of the Report 7
3.0 QUALITY ASSURANCE 8
4.0 INTRODUCTION 9
5.0 METHODS AND MATERIALS 12
5.1 Implementing Procedures (IPLVs), Materials, and Equipment Used in the Study 12
5.2 Laser Ablation Method Development 12
5.3 Interaction of Aqueous U, Gd and Nd with Iron Shot and Iron (III) Oxide 13
5.3.1 Sample Naming Convention 14
5.3.2 Instrument Settings and Quantitation by LA-ICP-MS 14
5.3.3 ICP-MS Procedure for Solution Analyses 16
5.3.4 Evolution of pH during Corrosion of Iron Shot 16
5.3.5 Corroborative Surface Techniques (SEM and XRD) 16
5.4 Task ORD-RF-02 Samples 17
6.0 ASSUMPTIONS 18
7.0 RESULTS, DISCUSSION AND CONCLUSIONS 19
7.1 Laser Ablation Method Development 19
7.2 Corrosion Study of Iron Shot and Iron (III) Oxide with U, Gd, and Nd 23
7.2.1 LA-ICP-MS and Aqueous Concentration Results 23
7.2.2 Depth Profiles Using LA-ICP-MS 27
7.2.3 Evolution and Influence of pH during Corrosion 29
7.2.4 Characterization of the Solids by XRD 32
7.2.5 Concentrations of U on the Surface of Iron Shot and Iron (III) Oxide 33
7.3 Task ORD-RF-O2 Samples 36
7.4 Conclusions and Recommendations based only on Q Data 41
7.5 Summary of Corroboration Including UQ Data 42
8.0 INPUTS AND REFERENCES 43
8.1 Inputs 43
8.2 Cited References 44
9.0 SOFTWARE 45
10.0 ATTACHMENTS 45

ABBREVIATIONS, ACRONYMS, AND SYMBOLS

DOE:	United States Department of Energy
HRC:	Harry Reid Center for Environmental Studies
ICP-MS:	Inductively Coupled Plasma Mass Spectrometry
IPLV:	Implementing Procedure Las Vegas
NA:	Not Available or Not Applicable
NIST:	National Institute of Standards and Technology
NSHE:	Nevada System of Higher Education
NTS:	Nevada Test Site
QA:	Quality Assurance
RSD:	Relative Standard Deviation
SMF:	Sample Management Facility
SN:	Scientific Notebook
UCCSN:	University and Community College System of Nevada
UNLV:	University of Nevada Las Vegas
UQ:	Unqualified Data

ACKNOWLEDGMENTS

Funding for this project was provided by the U.S. Department of Energy through a cooperative agreement (DE-FC28-04RW12237) with the UNLV Research Foundation, who issued a subcontract with the Harry Reid Center for Environmental Studies. The author thanks Vern Hodge, Ken Czerwinski, Amy Smiecinski, and Julie Bertoia (UNLV) for comments on a draft of this report.

STUDY TEAM

James Cizdziel, Yixin Wei, Caixia Guo, Tatjana Jankovic
Harry Reid Center for Environmental Studies
University of Nevada Las Vegas

Kaveh Zarrabi
Department of Physical Sciences
Community College of Southern Nevada

LIST OF TABLES

Table 1: Sample information for iron shot and iron oxide corrosion study.

Table 2: Laser and ICP-MS Experimental Settings.

Table 3: Laser spot size versus crater size in study sample matrices.

Table 4: Estimated Uranium Concentrations for the Surface of Fe Shot after 200 hours.

Table 5: Estimated Uranium Concentrations for the surface of Fe_2O_3 particles after 200 hours.

LIST OF FIGURES

Fig. 1 Image of the surface of an iron chip corroded with a solution containing uranium.

Fig. 2 Normalized uranium signal for ablation of the corroded iron shown in Figure 1.

Fig. 3 Uranium and Fe signal (TOF ICP-MS) for laser firings into the colored regions of the sample shown in Figure 1.

Fig. 4 Contents of ablation cell (looking from above) showing NIST glass standard reference material (large circular shapes in upper half of figure) and Fe-shot sub-samples (lower half of figure) arranged according to sample number and time period.

Fig. 5 Dimensions of a typical Fe-shot and an ablation crater.

Fig. 6 Aqueous concentrations of U, Gd and Nd during corrosion of Fe-shot.

Fig. 7 LA-ICP-MS signal for U (left) and Gd (right) for Fe-shot showing an increase in intensity as a function of reaction time (listed above peak).

Fig. 8 U signal for repetitive ablation at the same location showing a psuedo-depth profile at 0.2 hours (left) and 200 hours (right).

Fig. 9 Evolution of pH for a solution containing U, Gd and Nd after interaction with Fe-shot and Fe(III)Oxide.

Fig. 10 LA-ICP-MS signal showing the pH dependence on the affinity of U for solid Fe (III) oxide (left) and Fe shot (right) after 200 hours.

Fig. 11 XRD spectra of corrosion product sloughed off Fe-shot (sample 5-550) and captured on 0.45 micron filter.

Fig. 12 XRD spectra for sample 15-550 showing peaks characteristic of hematite, the starting material.

Fig. 13 U, Gd, and Nd signals from the ablation of Fe-shot from various reaction mixtures after 200 hours.

Fig. 14 U, Gd, and Nd signals from the ablation of Fe(III)Oxide from various reaction mixtures after 200 hours.

Fig. 15 ICP-MS Si signal within (left) and among (right) samples.

Fig. 16 ICP-MS signal showing poor reproducibility for Fe (left) and U (right) within a sample.

Fig. 17 ICP-MS U signal showing variability among samples. The samples were analyzed in reverse order (right side) but generally show the opposite pattern despite internal variability.

Fig. 18 ICP-MS Fe signal showing variability among samples. The samples were analyzed in reverse order (right side) and generally show the opposite pattern. Also the pattern is seemingly opposite to that of U in Fig. 17.

2.0 PURPOSE, SCOPE AND ORGANIZATION OF THE REPORT

2.1 Purpose

The purpose of this report is to summarize the work and present conclusions of Project Activity Task ORD-RF-03 conducted under cooperative agreement number DE-FC28-04RW12237 between the U.S. Department of Energy and the Nevada System of Higher Education (NSHE). The work was conducted in the Harry Reid Center for Environmental Studies of the University of Nevada Las Vegas from October 1, 2004 to September 30, 2006.

The purpose of the study was to develop a method using laser ablation inductively coupled plasma mass spectrometry (LA-ICP-MS) for the direct analysis of iron corrosion products, to evaluate its capabilities, advantages, and limitations, and to apply the method to examine the interaction of actinides, and other elements relevant to the long-term geologic storage of nuclear waste, with iron corrosion products. The desired quantification is for specific (targeted) sections of the surface; elemental ratios can be determined from the data if of interest.

2.2 Scope

The scope of this work includes documentation of the study's purpose, methods, results, conclusions, recommendations, and intended use.

2.3 Organization of the Report

Section 1 provides the table of contents and lists abbreviations, acknowledgments, study personnel, tables and figures. Section 2 discusses the purpose and scope of the report. Section 3 provides specific quality assurance information. Section 4 presents a brief introduction to the subject and other relevant background information. Section 5 focuses on the analytical methodology employed in the study. Section 6 fulfills a QA requirement to list assumptions used in the study. Section 7 consists of the results, discussion, and conclusions. Section 8 lists inputs (source data) and references cited in the report.

3.0 QUALITY ASSURANCE

The work described here was subject to the NSHE Quality Assurance (QA) Program requirements. This section provides an overview of the QA program used in this study, specific QA procedures and other program information can be found at the following website: http://hrc.nevada.edu/QA/. In addition, QA data are also documented in the scientific notebooks and at relevant locations within this technical report. No conclusions of this report are based on unqualified data.

Determination of precision and accuracy of the analytical measurements were described in each corresponding implementing procedure. Generally, precision was addressed through the use of laboratory replicates, and accuracy was evaluated using initial and continuing calibration verifications and analysis of standard reference materials (where applicable). Calibration standards were purchased directly from NIST or qualified vendors. No software or models were developed in this study. Balances and pipettes were calibrated annually by a qualified supplier or in-house using approved implementing procedures. Scientific notebook UCCSN-UNLV-086 Vol. 1 was used to document the research.

4.0 INTRODUCTION

Knowledge of the transport and fate of radionuclides in the environment is important to the Yucca Mountain Project (YMP), a large-scale effort designed to study the feasibility and predict the performance of a geologic repository for the nation's high-level nuclear waste. Understanding and predicting the behavior and movement of key elements, particularly the actinides, in the proposed repository and surrounding southern Nevada environment is difficult and requires a multidisciplinary approach. Funding for this project was provided by the U.S. Department of Energy through a cooperative agreement (DE-FC28-04RW12237) with the UNLV Research Foundation, who issued a subcontract with the Harry Reid Center for Environmental Studies (HRC). Researchers at the HRC examined two key fate and transport issues: the potential impact of microorganisms and the impact of the formation of alteration phases due to the corrosion of the waste package and waste forms on the chemistry, fate, and transport of radionuclides released from the site. The work was broken up into three tasks. Task ORD-RF-01 was focused on the influence of microorganisms. Task ORD-RF-02 involved surface complexation and solid dissolution studies. Task ORD-RF-03 (this study) entailed method development and elemental characterization of iron corrosion products, some of which were generated in task ORD-RF-02. For the purposes of this report iron alteration phases refers to any of a number of minerals (e.g., goethite) that can be formed when metallic iron is "altered" through oxidation processes.

Laser Ablation Inductively Coupled Plasma Mass Spectrometry (LA-ICP-MS) is a powerful analytical technique that focuses a laser beam on a target and sweeps vaporized and ablated material into an ICP-MS where elemental and isotopic information can be obtained. The spot size of the laser (and resultant ablation craters) can be adjusted down to a few micrometers in diameter making the method particularly effective in microanalytical applications. For example, the laser can target minute features of subsurface rock, such as secondary minerals, and repetitive sampling (firing) can provide depth profiles of the elemental and isotopic composition of samples. Consequently, LA-ICP-MS has become established as a very efficient and sensitive technique for the analysis of solids (Pickhardt et al. 2002).

LA-ICP-MS has also been used for the determination of long-lived radionuclides in solid nuclear waste or contaminated environmental samples (Becker 2000). However, in a review by Becker (2002) reporting on the state-of-the-art and progress in precise and accurate isotope ratio measurements by LA-ICP-MS, it was pointed out that despite the advantages of direct analysis of solids, the method only accounts for a few percent of published papers on the determination of isotopes. So the method is in its infancy and can benefit from further development and expanding applications.

Nevertheless, some literature relevant to the research on hand includes work by Leloup et al (1997) which improved the experimental setup for the analysis of impurities in U by LA-ICP-MS. Seltzer (2003) used LA-ICP-MS to measure U isotope ratios in depleted U contaminated soils. Vors et al. (2004) used a time-of-flight MS in combination with LA for measurement of isotope ratios employing a U vapor beam with photoionization. Becker and Dietze (2004) discuss precise and accurate isotope ratio measurements, including U by LA-ICP-MS using a multiple

collector system. With respect to iron and iron corrosion products, Devos et al. (2000) used LA-ICP-MS for spatially resolved trace analysis of archaeological iron finds. Weis et al. (2004) characterized ablation and aerosol generation during LA-ICP-MS with glasses with different iron oxide contents. The reader is encouraged to conduct a literature search to obtain additional and more up to date information on the growing application of LA-ICP-MS.

This study focused on developing LA-ICP-MS for the direct analysis of iron corrosion products (alteration phases), and applying the method to examine the interaction of actinides, and other elements relevant to the long-term geologic storage of nuclear waste, with iron corrosion products. Radionuclides can sorb or enter the alteration phase either through inclusion during the dissolution of the waste form (fuel pellet, borosilicate glass, etc.) or via sorption to the alteration phase from groundwater. One goal of the study was to evaluate the advantages and limitations of the method with respect to the analysis of key radionuclides with alteration phases possibly formed during the corrosion of the waste forms, waste package, and structural materials. This information was sought to shed light on the potential speciation, transport and fate of radionuclides, especially actinides, in the repository environment.

The scope of this work covered development and application of LA-ICP-MS for the direct analysis of iron alteration phases for select actinides (uranium) and rare earth elements (gadolinium and neodymium). Under investigation was the sorption or inclusion of these elements (added to the system) with solid alteration phases. Using Fe-shot (~1.5 mm spheres of carbon steel) in addition to already formed distinct mineral phases (Fe_2O_3) was of interest because it better approximates real-world scenarios where corrosion products are formed in-situ. Moreover, Fe-shot was once considered for inclusion in the Fermi waste package design to fill void volume, and thus reduce the volume that can be filled with water, which can act as a neutron moderator. The theory was that Fe-oxides have a larger molar volume compared to reduced iron such that upon corrosion void volume in the waste package would be decreased. Moreover, the iron could potentially reduce the actinides to a less mobile form and the resultant iron oxides could serve to sorb actinides that may be released over time.

Rare Earth Elements (REEs) are often used as surrogates for trivalent actinides in environmental studies (Kim et al. 2006). Neodymium (Nd) was included in this study because of chemical similarities to some actinide species (e.g., trivalent amercium^{+3} and trivalent curium^{+3} (Johannesson et al. 2000), which are present in high-level nuclear waste. For example, Nd^{+3} has a similar valence charge and ionic radii as Am^{+3}, 0.104 nm vs 0.107 nm, respectively (Shannon, 1976). The solids studied included distinct iron minerals [iron (III) oxide], amorphous iron corrosion products formed in the laboratory, and samples from surface complexation studies (Task ORD-RF-02). X-Ray Diffraction (XRD) analyses were employed as a potential corroborative technique. Given the importance of pH (see below), it was monitored at select intervals during the corrosion process.

Four key processes can influence the behavior of uranium (U) in the environment: sorption, precipitation, reduction and incorporation into mineral phases. These mechanisms tend to retard the transport of U in aqueous systems. There are several studies that suggest the interaction of uranium (U) species with corrosion products of iron. These interactions include, but are not limited to, sorption of U species to rust materials (Dodge et al. 2002) and co-precipitation of U

species with iron oxyhydroxides (Duff et al. 2002). These processes could ultimately govern the behavior and movement of U species in the repository environment. In aged, U-contaminated iron-rich soils, uptake of uranium by iron oxyhydroxides may be significant. Duff et al. (2002) showed that close to 1% of total molar concentration of uranium could be incorporated into solids.

The pH of the solution also plays an important role in the fate of aqueous uranium and gadolinium (Hull et al. 2000, p. 42). Gadolinium (Gd) is an element that has been considered as a component in the waste package design as a neutron absorber in criticality considerations (Radulescu et al. 2000). Under low pH (~<6) and low pE (~<3.5) conditions, which can be expected from fast corroding steel, U may be relatively immobile (uranites); and under alkaline conditions, U may form soluble carbonate complexes from equilibration with the ambient atmosphere (Hull et al. 2000, p.3-4). These soluble species can then potentially leave the waste package at a rate that depends on water flow. The solubility of Gd is also dependent on pH, among other factors. Wood (1990) provides a review of the aqueous geochemistry of REE and associated speciation in natural waters.

5.0 METHODS AND MATERIALS

This section describes the materials, methods and experimental procedures used in this study. Section 5.1 lists the NSHE QA procedures employed during the course of the study. The remaining sections describe experimental details.

5.1 Implementing Procedures (IPLVs), Materials, and Equipment Used in the Study

IPLVs:

1. IPLV-003, "Analytical and Top Loading Balance Use", Rev. 2 and 3.
2. IPLV-009, "Measurement of Trace Elements in Water Samples by the Inductively Coupled Plasma Mass Spectroscopy (ICP-MS)", Rev. 2, 3, 4.
3. IPLV-012, "Measurement of Conductivity, Alkalinity and pH in water samples", Rev. 3.
4. IPLV-017, "Pipettor Use and Calibration Check", Rev. 2.
5. IPLV-080, "Qualitative and Semi-Quantitative Elemental Determinations of Solids using Laser Ablation Inductively Coupled Plasma Mass Spectrometry (LA-ICP-MS)

Materials:

Iron chips, 99.98%, product #267945, Lot #01810ED; Aldrich, Milwaukee, WI
Uranium solution, 10 ppm, Lot U10-65U; Spex Certiprep, SC
Gadolinium solution, 1 ppm, Lot U12-03GD; Spex Certiprep, SC
Neodymium solution, 1 ppm, Lot U12-84ND; Spex Certiprep, SC
Iron shot, carbon steel, ~1.5 mm diameter, 4.485 g/cm^3 density; Metaltec Steel Co., Canton, MI
Iron (III) oxide, 99.999%, Lot 05717PD; Aldrich, Milwaukee, WI
Ammonium hydroxide, high purity, Lot 7205060, SeaStar Chemicals, Seattle, WA
Nitric acid, high purity, Lot 1203050, SeaStar Chemicals, Seattle, WA

Equipment:

Analytical balance, Sartorius, R200D, S/N 30903489
LSX-500 and LSX-213 Laser Ablation Systems, Cetac Inc., Omaha, NE
Optimass 8000, TOF-ICP-MS, S/N 2055410, GBC Scientific Inc
Axiom, SF-ICP-MS, S/N 833, Thermo Electron Corp
PANalytical X'PERT Pro X-ray Diffraction Spectrometer, UNLV Department of Geoscience
JEOL, Scanning Electron Microscope, UNLV Department of Geoscience
Beckman 011 pH meter

5.2 Laser Ablation Method Development

The time-of-flight inductively coupled plasma mass spectrometer (TOF-ICP-MS) instrument was installed in March of 2005 and task personnel received advanced training the following month. Special attention was given to collecting and handling data associated with transient signals. Installation of the laser ablation unit, at the heart of this task, was delayed due to manufacturing difficulties with the laser crystal coating on the LSX-3000 unit (Cetac Inc., Omaha, NE). Due to time constraints, a different model (LSX-500) was installed in July of 2005. The LSX-500 was

used for Section 7.1 and 7.2.5, whereas an LSX-213 was used for section 7.2 (except 7.2.5) and 7.3. The LSX-213 provides a >4 mJ/pulse with a 5 ns pulse width, whereas the LSX-266 yields >9 mJ/pulse with <6 ns pulse width. Additional laser property details are available form the manufacturer (Cetac Technologies, Omaha, NE). Because the LSX-213 was used primarily for qualitative (bulk) analysis, we do not expect there to be any impact on the results between the two systems.

Several samples of iron chips (3-6 mm in diameter; see materials in Section 5.1) were allowed to react with 5 ml of a solution containing 10 ppm U. The reaction resulted in an irregular surface coating of variable color. The samples were gently washed for < 30 sec with deionzied water (>18 MΩ/cm) and air dried. The surface was used as a test specimen to study the influence of a number of LA and ICP-MS parameters on the sensitivity and stability of the elemental signal. Laser and ICP-MS parameters were systematically varied and the intensity of the signal for U and Fe was monitored.

5.3 Interaction of Aqueous U, Gd and Nd with Iron Shot and Iron (III) Oxide

In short, iron-shot (carbon steel) and iron (III) oxide (the most stable corrosion product) were "reacted" with groundwater obtained near Yucca Mountain (well J-12) which was spiked with U, Gd and Nd and modified to a pH of ~3 and 8. Subsamples of the liquid and solid were collected at set intervals thereafter. For the solid, U was analyzed by LA-ICP-MS. For the liquid, U, Gd and Nd were analyzed by ICP-MS. More specifically, iron shot and iron (III) oxide were reacted separately with 100 ml of solution containing variable pH (~3.5 and ~8.5) and concentrations (1 and 10 ppm) of uranium (U), gadolinium (Gd), and neodymium (Nd) made up in J-12 groundwater. The water from well J-12, located near Yucca Mountain, has been studied extensively over the years for a range of chemical parameters, including concentrations of trace elements. Table 1 summarizes sample information for the iron shot and iron oxide corrosion study. High purity nitric acid or ammonium hydroxide (SeaStar Chemicals, Seattle, WA) were added drop wise to reach the desired pH level. Elemental solutions were obtained from Spex Certiprep (Metuchen, NJ) with concentrations of 10,000 µg/ml (for U) and 1,000 µg/ml (for Gd and Nd).

The solid samples and solutions were allowed to interact (sitting passively) and sub-samples of the solids (several pieces of shot or oxide) were removed at 0.2, 2, 20 and the 200 hour intervals using Teflon-coated tweezers. The sub-samples were rinsed for a few seconds with D.I. water and allowed to air dry. The dried sample was then placed in labeled plastic bags until analysis. For the liquid, ~0.5 ml was drawn into a plastic syringe and filtered through 0.45 µm membrane into weighed 50 ml centrifuge tubes. The samples were stored in a refrigerator at ~4º C until analysis.

5.3.1 Sample Naming Convention

Sample descriptions are provided in Table 1. Sub-samples taken during the course of the experiments were labeled with the sample number followed by the "reaction" time (i.e., the period of time the pieces of solid or liquid were in contact with the other phase). For example, the Fe-shot removed after 200 hours from sample #5 was labeled as 5-200. One-hundred ml of solution was used for the study. Table 1 is presented as an overview; more exact concentration and pH data are presented in the Results Section. The masses for samples 7 and 8 differed in part to investigate the influence of starting mass in the experiment

Table 1. Sample information for iron shot and iron oxide corrosion study

Sample #	Solid Starting Material	Mass of Starting Material (g)	Initial Approximate Conc. U, Gd, Nd (ppm) in J12 Water	Initial Approximate pH
1	Fe-shot	41.6141	1	3.5
2	Fe-shot	42.9801	1	3.5
3	Fe-shot	44.9293	1	8.5
4	Fe-shot	44.3620	1	8.5
5	Fe-shot	42.1760	10	3.5
6	Fe-shot	43.8749	10	3.5
7	Fe-shot	45.0365	10	8.5
8	Fe-shot	15.7493	10	8.5
9	Fe-shot	22.5828	J12 water only	8.5
10	Fe-shot	20.9119	J12 water only	8.5
11	Fe_2O_3	0.5083	1	3.5
12	Fe_2O_3	0.4770	1	3.5
13	Fe_2O_3	0.2808	1	8.5
14	Fe_2O_3	0.2859	1	8.5
15	Fe_2O_3	0.3496	10	3.5
16	Fe_2O_3	0.3086	10	3.5
17	Fe_2O_3	0.3060	10	8.5
18	Fe_2O_3	0.3139	10	8.5
19	Fe_2O_3	0.3234	J12 water only	8.5
20	Fe_2O_3	0.3359	J12 water only	8.5

DTN: R03JC.003

.

5.3.2 Instrument Settings and Quantitation by LA-ICP-MS

Quantitation was performed using the GBC Optimass TOF ICP-MS. Experimental settings for the laser and the Time-Of-Flight ICP-MS are given in Table 2. The laser was fired using a single shot at full energy, 20 Hz, ~200 µm spot size (diameter), with a 30 sec delay between samples (unless otherwise noted). The conditions were determined by monitoring masses 57, 146, 158,

and 238, on the ICP-MS for Fe, Nd, Gd, and U, respectively, and adjusting the parameters for stability and sensitivity. ICP-MS settings, such as gas flows and the torch position, were optimized daily using a line scan of NIST glass. The primary laser-based parameters available for selection are the laser pulse repetition rate (Hz): 1, 2, 3, 4, 5, 10, 20; spot size (µm): 10, 25, 50, 100, 150 and 200; and energy: increments of 5% from 5% to 100%. A complete documented systematic study of these parameters on the signal intensity was not conducted because the it was determined that using these maximum laser settings (except for number of shots) yielded the most intense signals, and this was considered beneficial for potential quantitation. Note: in the interest of time, we moved on to attempting quantitation rather than further scrutinize these parameters.

Later in the study, samples of Fe-shot and Fe(III)oxide were re-examined (qualitatively) by LA-ICP-MS using a sector-field ICP-MS (Axiom), which has greater sensitivity than the time-of-flight instrument. Exact analytical masses monitored by the Axiom were 57.935, 141.908, 157.924, 238.051 for Fe, Nd, Gd, and U, respectively. The Axiom is a high resolution instrument and provided masses to greater precision than does the Optimass. The Axiom was used primarily with the LSX-213. Because of the greater sensitivity of the magnetic sector ICP-MS compared to the TOF-ICP-MS, a less abundant isotope was used for Fe, the primary matrix element. For Nd, the more abundant isotope was monitored for greater sensitivity. Interference from an isotope of Ce with the same nominal mass was not expected to be a problem because a single element standard was used for Nd. In summary, quantitative data was only generated using the TOF-ICP-MS; because of time and the variability observed in the TOF-ICP-MS LA data, the Axiom was used only in a qualitative manner.

Table 2. Laser and ICP-MS Experimental Settings

Parameter	Setting
Laser Energy	Full
Laser Repetition (Hz)	20
Spot Size (µm)	200
Delay between samples (sec)	30
Mass monitored	57, 146, 158 and 238

Gas flows and torch position were optimized daily. Non-Q, for informational purposes only. DTN: R03JC.003

Quantitative measurements were attempted on the Fe-shot samples using IPLV-080, "Qualitative and Semi-Quantitative Elemental Determinations of Solids using Laser Ablation Inductively Coupled Plasma Mass Spectrometry (LA-ICP-MS)". Details of this procedure can be found on the Harry Reid Center for Environmental Studies, Quality Assurance website at: http://hrcweb.nevada.edu/qa/IPLV/IPLV-080.pdf. In short, instrumental blank (background) measurements were collected without firing the laser. Then, NIST glass standards (SRM 612, 614 and 616) were used for calibrating the instrument (when certified concentrations were available). Samples were analyzed using the same conditions (ablation and ICP-MS parameters) as the standards. A NIST standard was run at the conclusion after all samples have been analyzed for monitoring accuracy. Data was reduced in Excel. Normalization using Fe was not

used because the Fe-signal was stable similar between samples. Quantification difficulties arise when using standards that are not matrix matched and these are discussed further in Section 7.

5.3.3 ICP-MS Procedure for Solution Analyses

Measurements of trace elements in solution were conducted using an ICP-MS. The procedure is detailed in implementing procedure, IPLV-009, and will not be discussed here. The procedures are available on the NSHE QA program's webpage at http://hrcweb.nevada.edu/qa/iplv.htm.

5.3.4 Evolution of pH during Corrosion of Iron Shot

A separate experiment was conducted to track pH changes as a function of corrosion time for Fe-shot and iron (III) oxide using the same four starting solutions and materials as the experiment described in Section 5.3. In short, ~30 ml of a solution containing 1 ppm of U, Gd and Nd (pH adjusted to 2.75) was added to ~10 g of Fe shot in a 50 ml centrifuge vial (time 0). Similarly, ~30 ml of 1 ppm of U, Gd and Nd (pH adjusted to 9.0) was added to ~10 g of Fe shot as before. Two vials were also prepared for iron (III) oxide. Exact weights and volumes were not recorded in this experiment because we were only interested in changes in solution pH. About 1 gram of the solid oxide was combined with 30 ml of a solution containing 10 ppm of U, Gd and Nd at pH of 2.70 and 8.86. These were the same solutions used in the prior experiment explained in Section 5.3. The pH was measured in the solution above the solid at 0.2, 2, 20, and 200 hour intervals using IPLV-012 Rev. 3, "Measurement of Conductivity, Alkalinity, and pH in Water Samples".

5.3.5 Corroborative Surface Techniques (SEM and XRD)

Iron chip corroded in the presence of aqueous uranium (Section 5.2) was analyzed by a scanning electron microscope housed at the UNLV Department of Geoscience for uranium content (UQ). In addition, select solutions (5-550, 7-550, 9-550, 15-550, 17-550 and 19-550) were filtered (0.45 μm) at 550 hours after the start of the experiment outlined above. These samples were chosen to represent low and high pH conditions for the Fe-shot, Fe-oxide, and associated blanks. Only the samples using high concentration were selected because it was believed that these would be the most likely to provide signals measurable by the less sensitive techniques. The filters, containing fine particulates and corrosion products sloughed off the solids (particularly for the Fe-shot), were allowed to air dry. The particulate matter was scraped off the filter and introduced into a PANalytical X'PERT Pro X-ray Diffraction Spectrometer located at UNLV's Department of Geoscience for analysis. Although enough material was present for XRD analysis, the concentration of U, Gd and Nd was too low to be measured (see results). This work is considered Non-Q, for information purposes only.

5.4 Task ORD-RF-02 Samples

As part of Task ORD-RF-02 precipitates containing variable amounts of U, Fe and Si were mixed with potassium bromide (KBr) and pressed into pellets for infrared spectroscopy. Subsequently the pellets were transferred to this study (Task ORD-RF-03) for evaluation by LA-ICP-MS. Six of these pellets (6-20, 6-20D, 6-23, 7.5-33, 9-40, and 9-68) were randomly selected for method development. If successful more samples were to be analyzed. The laser (LSX-213; Cetac Inc.) was coupled to a sector-field ICP-MS (Axiom) from VG Elemental (now Thermo Electron). The LSX-213 parameters were optimized prior to analysis. The Axiom was operated in single collector mode and the signal was monitored at mass 28.976 (Si), 57.935 (Fe) and 238.051 (U). The laser was operated at 20 Hz in full energy mode with a 200 micron beam width. A single laser shot was fired into the pellets at multiple locations. The vapors and particles generated by the ablation process were swept into the ICP-MS via an argon gas stream. A 30 sec delay was employed between shots to allow the signal to return to baseline levels.

6.0 ASSUMPTIONS

Both gadolinium and neodymium are rare earth elements with substantial chemical similarities. This report primarily discusses results for gadolinium and assumes that neodymium would behave in a similar manner. The reasons both elements were used for this study are given in the Introduction. A single laser ablation shot was used for most of the work herein because it was assumed we were dealing with a surface phenomena and a single shot would be the least invasive (produce the shallowest crater) to maximize analyte signal relative to the underlying matrix. Correlations of laser spot size and ablated area are assumed to be unity.

7.0 RESULTS, DISCUSSION AND CONCLUSIONS

7.1 Laser Ablation Method Development

As detailed in Section 5.2, several samples of iron chips were allowed to react with a solution containing uranium. The reaction resulted in an irregular surface coating of variable color (Fig. 1). The corroded sample was gently washed with distilled water, air dried, and used for studying the influence of a number of LA and ICP-MS parameters on the sensitivity and stability of the elemental signal. Experimental details are documented in scientific notebook UCCSN-UNLV-086 Vol. 1. For this material it was found that a single laser ablation shot was sufficient to produce a large reproducible signal for U. Consequently multiple shots were not necessary. The effect of multiple shots is examined in Section 7.2.2. Later in the study, when a sector field ICP-MS was used, a single laser ablation shot was enough to produce a large enough signal for analysis. A single laser shot was also chosen because it constitutes one of the least invasive ablation and we expected to be dealing with primarily surface chemistry. However, the disadvantage of using a single shot for analysis is that the composition of the ablated area may not reflect an averaged surface sample if heterogeneities are present. The following optimized laser instrument parameters were identified: 100% energy (E), 1 Hz, and 50 μm spot size. Note: these are minimum settings available, except for E. Energy units are not defined, however, the manufacturer states that there is ~4 mJ/pulse. Using a 50 μm spot size was better than a 10 μm spot size because unlike the 10 μm spot it also generated a decent sized Fe signal for which the U could be normalized (Fig. 2). Line scans were not appropriate for the Fe-shot (described later) because the rounded surface.

Signal normalization is important because different alteration phases (mineral structures) are likely to ablate (absorb energy) differently, resulting in variable amounts (masses) of material reaching the plasma. Indeed, the Fe-normalized data is somewhat different and more uniform than the un-normalized U data. For our test specimen, it appears that the lighter white colored areas contain relatively greater U content than the other regions. Conversely, the gray regions, which appear to be areas where the underlying Fe solid is exposed or possibly where the oxide coating has flaked off the surface, consistently appear to generate the lowest U signal (Figs. 2 and 3). Scanning electron microscope (SEM) measurements (non-Q) corroborated that the lighter regions contained higher U concentrations compared to the darker regions on the same sample (SN-UCCSN-UNLV-086 Vol. 1).

Normalization was conducted for matrix and drift correction as follows. A matrix element (e.g., Fe for iron oxides) was monitored along with the analyte elements (e.g., U, Gd, Nd). The analyte signal was divided by the signal for the matrix element (peak heights were used) to yield a relative (normalized) signal. This was done, for example, for the data presented in Fig. 2 because of the variability in the Fe-signal and because in the surface was visibly heterogeneous (see Fig. 1). However, later in the study normalization was not used because there was little, if any, variability in the Fe signal for the Fe-shot samples.

Thus, in addition to determining optimal ablation and measurement parameters, it was shown that LA-ICP-MS is useful in obtaining elemental data on specific corrosion areas (down to the 50

micron level). Because the technique can estimate actinide uptake on the microscale, it may be useful as a screening tool to identify those that may require more costly surface characterization techniques. The time-of-flight (TOF) instrument has the advantage of quasi-simultaneous elemental data for normalization purposes. The multiple collector ICP-MS is not capable of such measurement given the wide dispersion in masses (Fe-57 & U-238).

Given these results, a method was formalized and approved in accordance with the NSHE QA Program. The procedure (IPLV-080) describes a technique used for the determination of elements in solids using Laser Ablation Inductively Coupled Plasma Mass Spectrometry (LA-ICP-MS). The IPLV was devised specifically for analyses of samples associated with this task, including well defined mineral phases, such as goethite and magnetite, and poorly characterized corrosion products, such as amorphous iron-containing alteration phases. However, the method could be readily modified for other solid environmental or geological samples. Elements and isotopes chosen for analysis would depend on the purpose of the analysis and the availability of qualified standards.

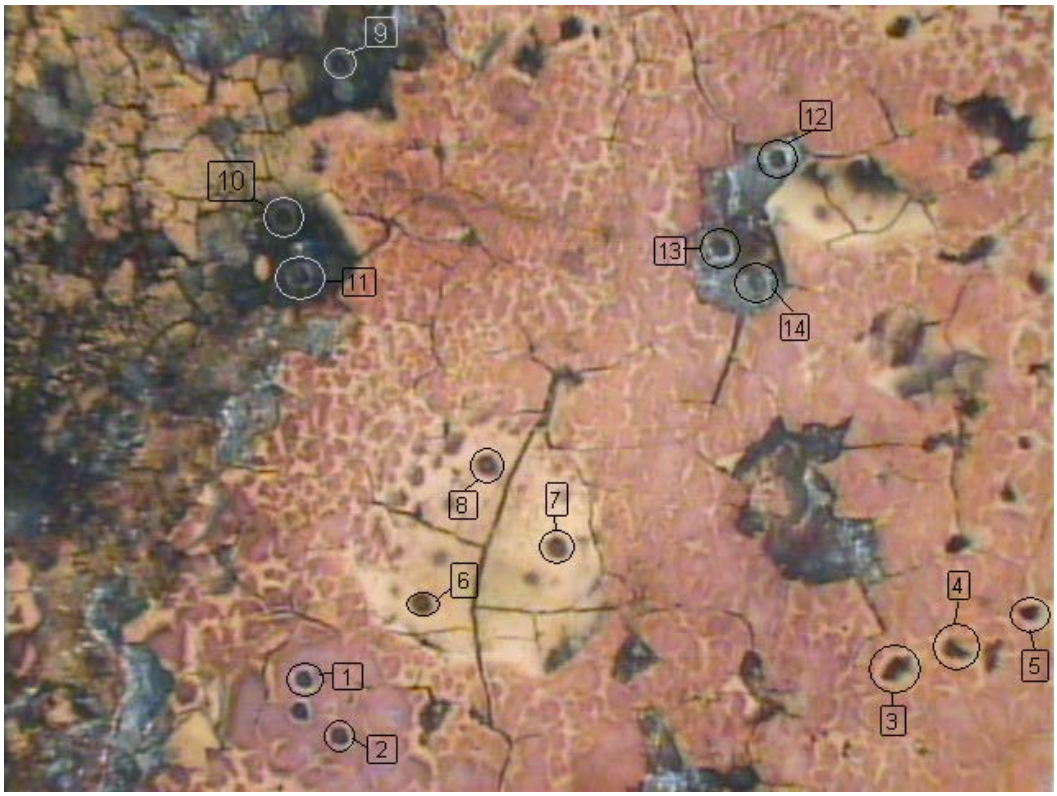

Figure 1: Image of the surface of an iron chip corroded with a solution containing uranium. Dark circular spots are ablation craters about 50 microns in diameter. Numbers correspond to peak numbers shown in figure 3. Non-Q, for informational purposes only.

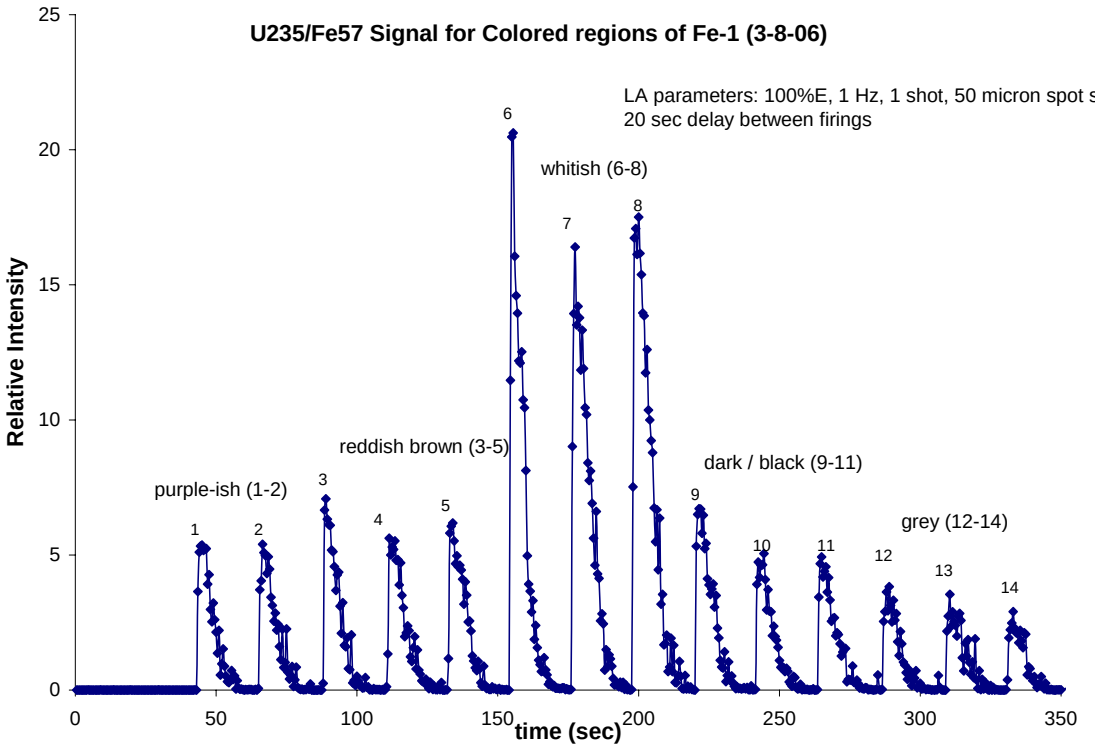

Figure 2. Normalized uranium signal from the TOF ICP-MS for ablation of the corroded iron shown in figure 1. Peak numbers match numbered ablation craters in figure 1. Non-Q, for informational purposes only. Source: SN-UCCSN-UNLV-086 Vol. 1.

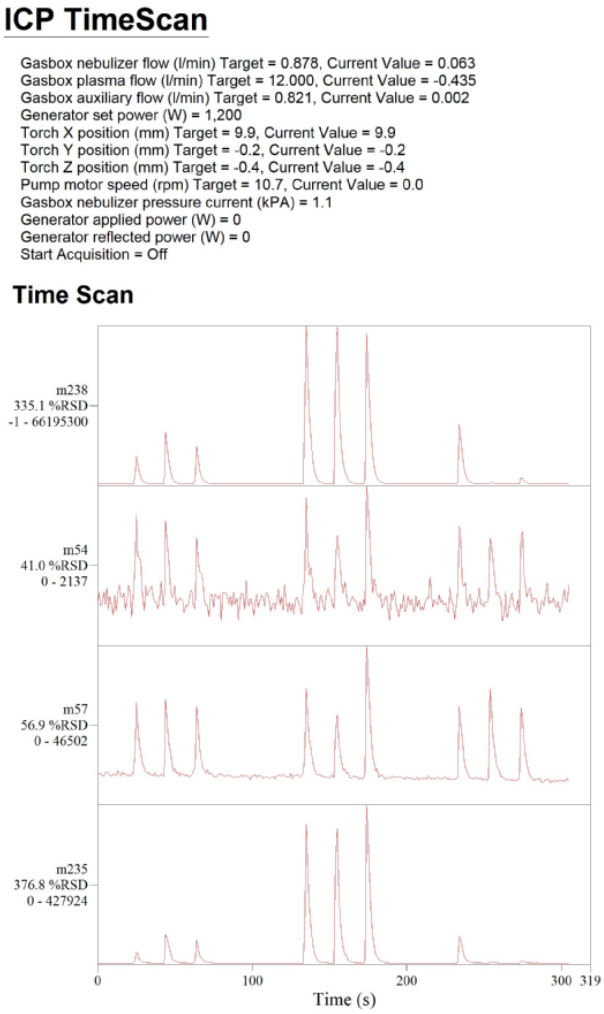

Figure 3. Uranium and Fe signal (TOF ICP-MS) for laser firings into the colored regions of the sample shown in Figure 1. The first three peaks (0-100 sec) correspond to a purple colored region, the tall middle three peaks (100-200 sec) represent a white colored region, and the last peaks (200-300 sec) are associated with grey and dark areas. The masses monitored (top to bottom) are 238 (U), 54 (Fe), 57 (Fe) and 235 (U). ICP-MS parameters are also displayed. Non-Q, for informational purposes only. Source: SN-UCCSN-UNLV-086 Vol. 1.

7.2 Corrosion Study of Iron Shot and Iron (III) Oxide with U, Gd, and Nd

7.2.1 LA-ICP-MS and Aqueous Concentration Results

After gaining experience and developing methods using the test specimen (Section 7.1), an experiment was conducted to study the behavior of U, Gd and Nd in an actively corroding system. Fe-shot (~1.5 mm spheres of carbon steel) was used to better approximate real-world scenarios where corrosion products are formed in-situ. Iron (III) oxide (Fe_2O_3) was also investigated (separately) using the same experimental matrix because others have studied this end mineral extensively albeit under different experimental conditions (e.g., Moyes et al. 2000). Gadolinium was included in the experiment because Gd was considered as a component in the waste package design as a neutron absorber in criticality considerations. Neodymium was included because of chemical similarities to some actinide species (Am^{+3} and Cm^{+3}).

Details of the experiment are presented in Section 5.3. In short, iron shot and Fe_2O_3 were mixed separately with a solution containing U, Gd, and Nd in J-12 groundwater at variable pH (~3.5 and ~8.5) and concentrations (1 ppm and 10 ppm). Pieces of the solid were removed from the reaction mixtures at 0.2, 2, 20 and 200 hour intervals (after the start of the reaction), rinsed with deionized water, and analyzed using LA-ICP-MS. Sub-samples of the solution were also collected at the same time intervals and analyzed by ICP-MS. Total mass of each element introduced in our experiment is the sum of the amount in solution, adsorbed, precipitated or co-precipitated.

Figure 4 shows the contents of the ablation cell (looking from above) including NIST glass standard reference material and spheres of Fe-shot arranged according to sample number (1-12) and time period (0.2, 2, 20, and 200 hours). Figure 5 presents a magnified view of a piece of Fe-shot showing a typical ablation crater.

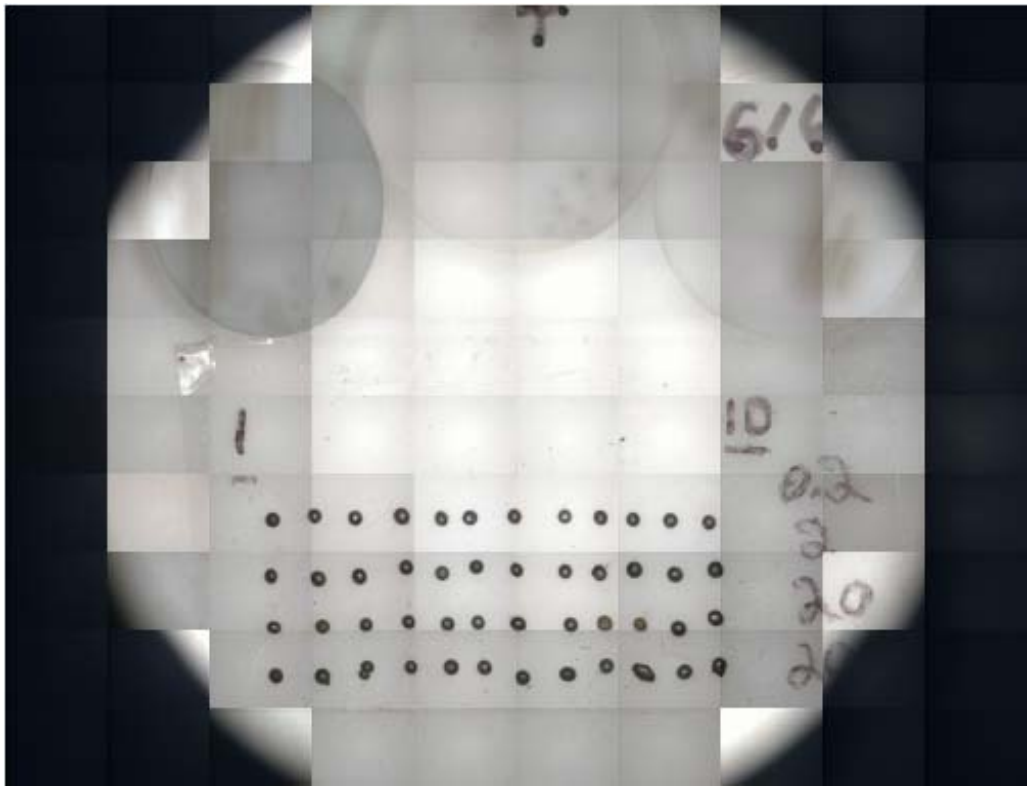

Figure 4: Contents of ablation cell (looking from above) showing NIST glass standard reference material (large circular shapes in upper half of figure) and Fe-shot sub-samples (lower half of figure) arranged according to sample number and time period. Non-Q, for informational purposes only.

Figure 5: Dimensions of a typical Fe-shot and an ablation crater. Non-Q, for informational purposes only.

For Fe-shot experiments at "low" initial pH (pH 2.70), the aqueous concentration of all three elements (U, Gd, Nd) decreased in the solution with time (Fig. 6, Nd not shown). Aqueous concentrations were determined by ICP-MS as discussed in Section 5. Correspondingly, the ICP-MS signal associated with the surface of the solid increased with time (Fig. 7, Nd not shown). Each peak in Figure 7 is associated with an ablation event on an individual piece of Fe-shot removed from the reaction at the specified time.

The concentration of U, Gd and Nd in the "high" initial pH solutions (pH 8.86) was already significantly below that of their low pH counterparts at 0.2 hours (Fig. 6, Nd not shown). Under the study conditions these elements are less soluble at these higher pH levels. Nevertheless, there still appears to be a decrease in the aqueous concentration with time in this actively corroding system.

Because the mass of the solid and the amount of U added are known quantities, a rudimentary mass balance for the system was attempted. However, surface areas were not measured and the mass transported during ablation or crater depths were not determined, and this hindered the analysis. Although some assumptions can be made for the calculation, such a spherical shape for the Fe-shot and uniform density and crater depths for the samples, there were too many assumptions and unknowns to obtain meaningful results.

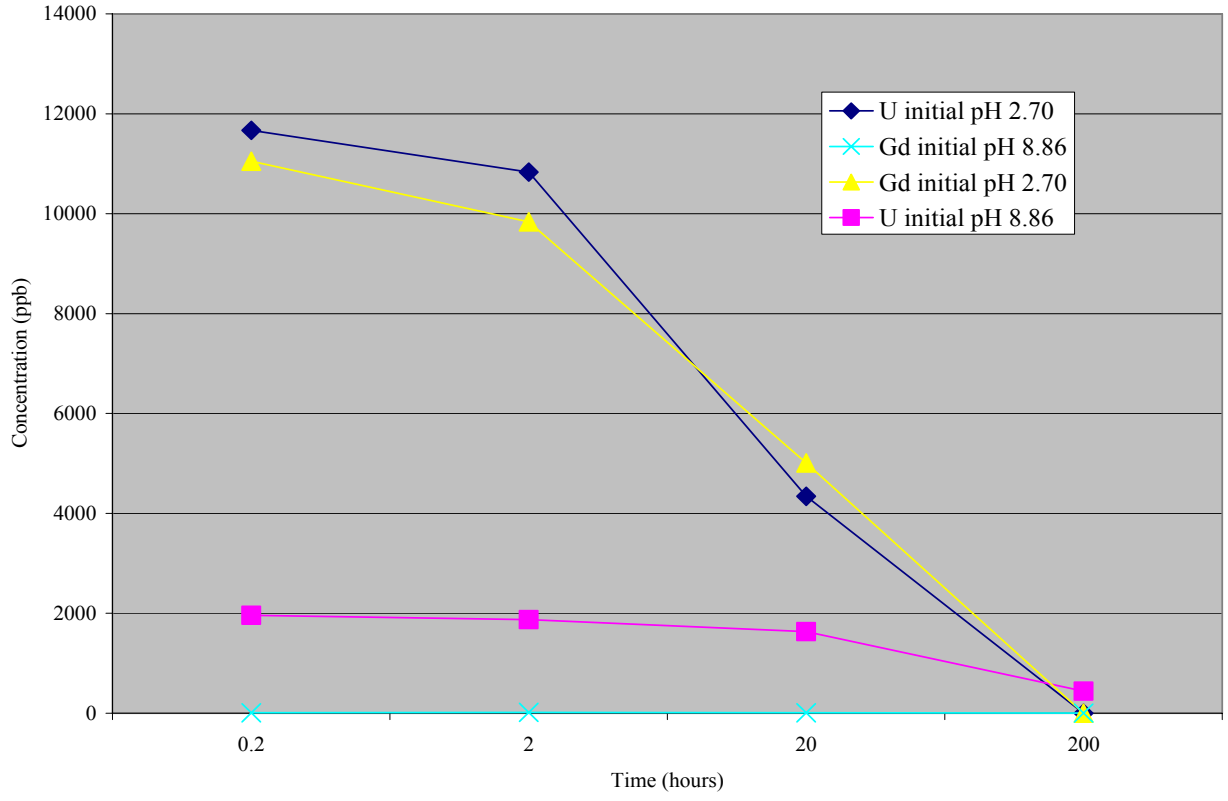

Figure 6. Aqueous concentrations of U and Gd during corrosion of Fe-shot. The starting solution was ~10 ppm. pH values were measured in the solution prior to adding to the solid. pH was not monitored but is addressed in a separate experiment under similar conditions in Section 7.2.3. Note the x-axis employs a logarithmic scale and error bars (1 SD) fall within the markers. DTN: R03JC.002.

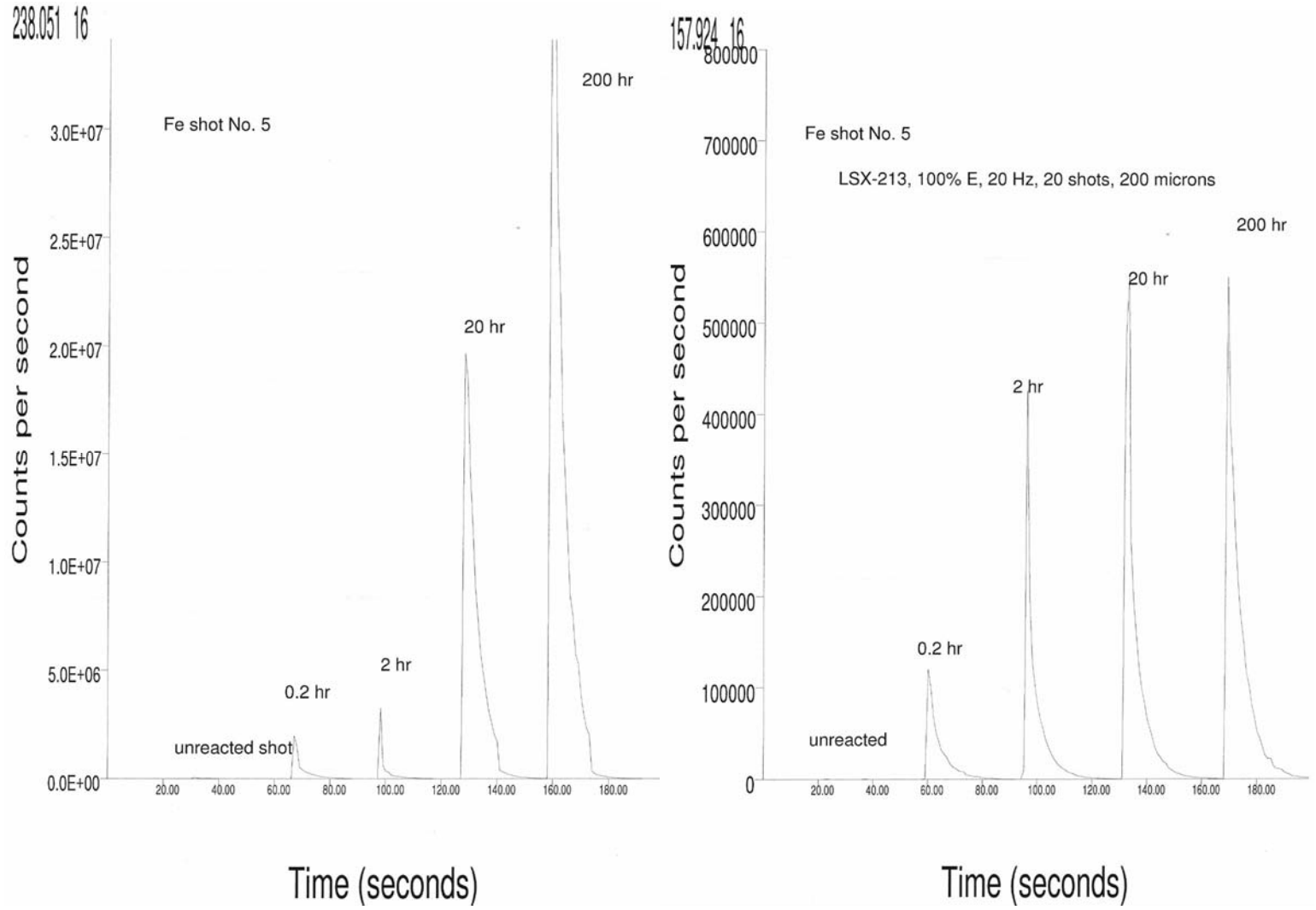

Figure 7. LA-ICP-MS signal for U (left) and Gd (right) for Fe-shot showing an increase in intensity as a function of reaction time (listed above peak). The bottom time scale is for the instrument scan and is not relevant. The initial solution pH and U concentration was ~3.5 and 10 ppm, respectively. Laser ablation parameters are listed in upper right. LSX-213 is the laser ablation instrument model number. Non-Q, for information purposes only. Source: SN-UCCSN-UNLV-086 Vol. 1.

7.2.2 Analyte Removal from Surface Using LA-ICP-MS

Analyte removal from the surface was accomplished by repetitive ablation at the same spot and monitoring the elemental signal. Time was provided between ablation events to allow the signal to return to background. In theory, each ablation event would remove additional material increasing the depth of the crater proportionally. However, in practice some material is not fully removed and condenses around and within the pit (Gunther et al. 2003). In addition, physically removing material from the pit becomes more difficult as the depth increases. Nevertheless, we observed differences for Fe-shot at 0.2 hours compared to that at 200 hours (Fig. 8 for U, Gd and Nd not shown but had similar behavior). As anticipated the signal decreased with each ablation event, however the decrease was greater for the 0.2 hour sample relative to the 200 hour sample. Considering the increase in signal with time presented earlier, it is likely that the difference reflects a greater deposition at 200 hours versus 0.2 hours. This is an example of how LA may be useful as a screening tool to identify those samples with sufficient analyte on the surface before more costly surface characterization techniques are employed.

The relationship between laser spot size and crater diameter was examined by ablating the four primary sample matrices used in the study and subsequently measuring the crater diameter via a feature of the LA software. The results and LA conditions for this work are listed in Table 3. The crater diameters were consistent between the three replicate ablation events, with relative standard deviations generally less than 10%. Moreover, the crater size was usually within 10% of the selected laser spot size.

Table 3. Laser spot size versus crater size in study sample matrices.

Matrix	Selected laser spot size (μm)	Approximate crater diameter size (n=3)		
		mean (μm)*	SD	Relative SD
Fe-shot	50	51	2	3
	100	108	4	3
	200	194	17	9
Fe (III) oxide	50	61	13	22
	100	109	9	8
	200	209	9	4
KBr pellet	50	60	2	3
	100	110	10	9
	200	186	8	4
Fe-chip	50	62	2	3
	100	111	5	4
	200	196	5	3

Non-Q, for informational purposes only. *Measured by a feature in the LSX-213 software. Other laser parameters: 100% E, 20 Hz, 100 shots. Note: because of the irregular surface, particularly for Fe-shot and Fe-oxide, measured crater diameters are approximate. Due to the transparency of the KBr pellet, multiple shots were required to visually observe the crater. Source: SN-UCCSN-UNLV-086 Vol. 1

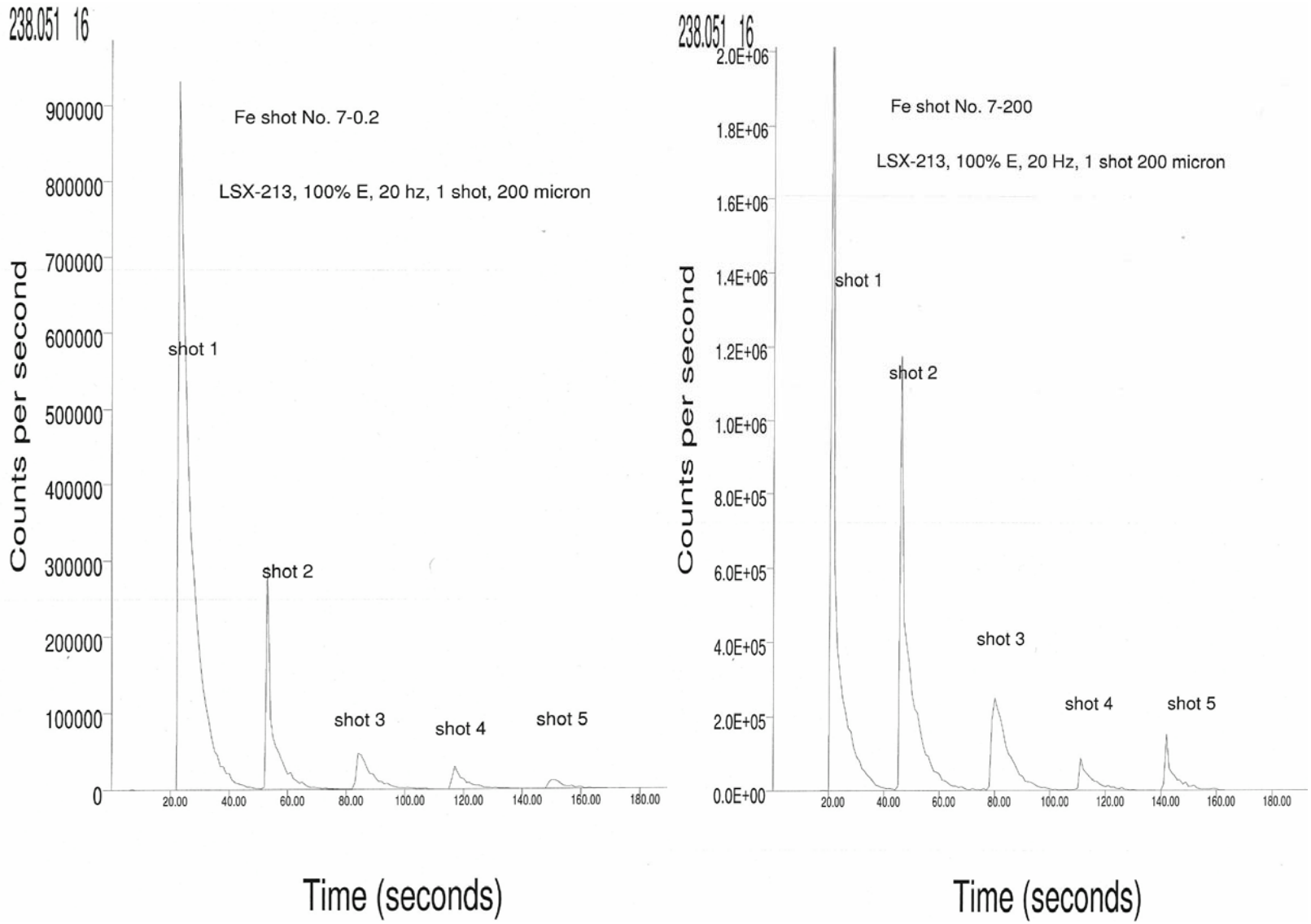

Figure 8. U signal for repetitive ablation at the same location showing a psuedo-depth profile at 0.2 hours (left) and 200 hours (right) for sample #7. Note that the 200 hour specimen shows a larger overall signal (counts per second, y-axis) and a smaller relative decrease with each laser firing (shots 2-5). Non-Q, for informational purposes only. Source: SN-UCCSN-UNLV-086 Vol. 1.

7.2.3 Evolution and Influence of pH during Corrosion

An experiment was conducted to track pH changes as a function of corrosion time for Fe-shot and Iron (III) oxide at a “low” starting pH (~3.5) and a "high" initial pH (~8.5). Results are presented in Figure 9. For the sample containing iron (III) oxide, the pH remained relatively unchanged, except for an initial small drop for the high pH solution. More interestingly, the pH for the solutions containing the Fe-shot had significant and steady pH increase. The pH climbed from <3 to >10 for the solution associated with the Fe-shot sample that started at low pH. This is an enormous change in hydrogen ion concentration. In contrast, the pH of the solution starting at a “high” pH initially dropped (similar to the oxide) but then steadily increased over time. The solutions contained 1 ppm U, Gd, and Nd (see Section 5.3.4).

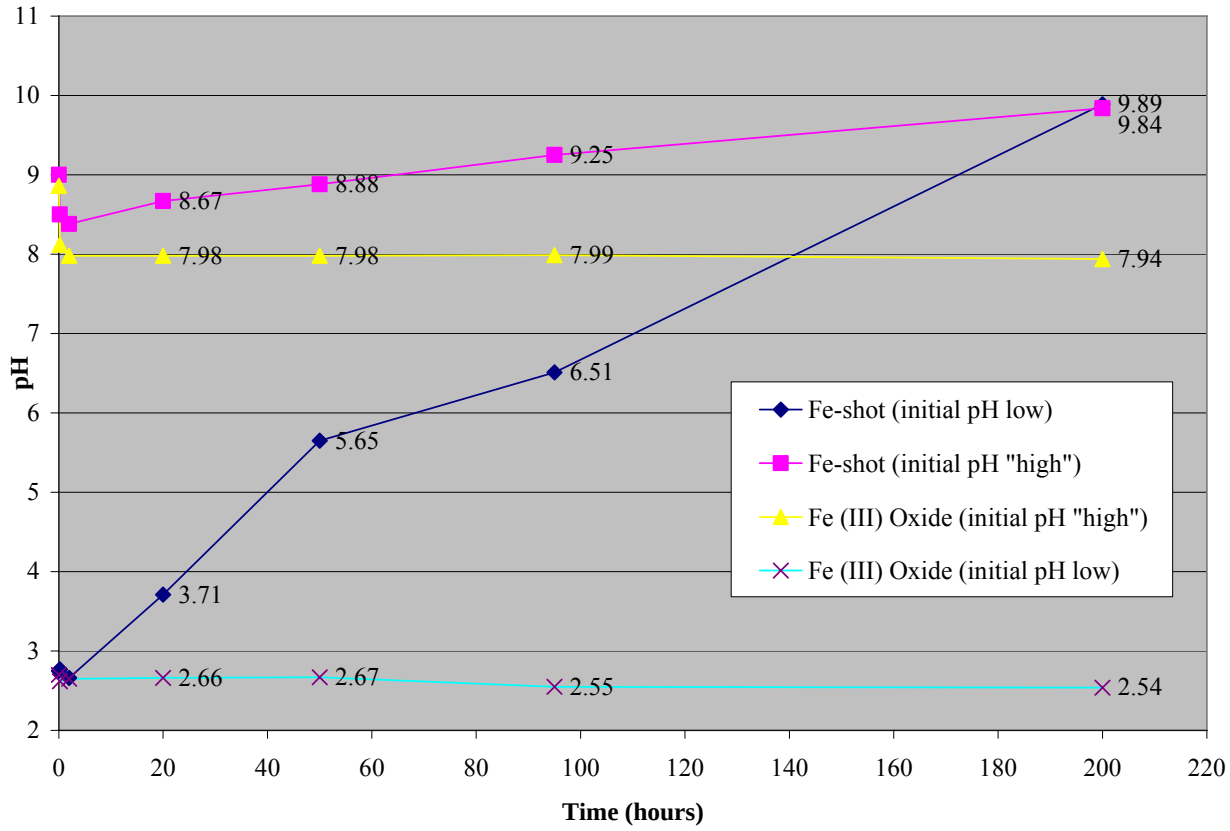

Figure 9. Evolution of pH for a solution containing U, Gd and Nd after interaction with Fe-shot and Fe(III)Oxide. Note that the lines are not fit with a mathematical function but simply connected between points. The initial pH values were 9.00 and 2.77 for Fe-shot and 8.86 and 2.70 for Fe (III) Oxide. At 0.2 hours the pH values were 8.50 and 2.77 for Fe-shot and 8.12 and 2.62 for Fe (III) Oxide. At 2 hours the pH values were 8.38 and 2.66 for Fe-shot and 2.65 and 7.98 for Fe (III) Oxide. The remaining values are provided on the graph. DTN: R03JC.001.

With changes observed in Fig. 9, the data from the Axiom becomes more understandable. For example, the affinity of U and Gd for solid Fe (III) oxide is partly dependent upon solution pH. Figure 10 (left side) shows that the elements stay in solution and are minimally sorbed to the

solid at “low” pH (peak labeled 15-200), whereas at “high” pH (~8) the elements are incorporated onto the surface of the oxide (as evidenced by the huge center peak labeled 17-200). In contrast, after the same period of time (200 hours) Fe-shot had high levels of the elements associated with solid for both solutions, including the “low” pH solution (5-200 and 7-200 in the figure). The different behavior for the “low” pH solution between the Fe (III) oxide Fe-shot (Fig. 10) can be seen explained by Fig. 9. After 200 hours the “low” pH sample is no longer at “low” pH but has become more like the high pH solution, thus the LA-ICP-MS scans (peaks 7-200 and 5-200 on the right side of Fig. 10) are alike. The influence of pH and other key geochemical parameters on uranium interactions with mineral surfaces are described by Pabalan et al. (1998).

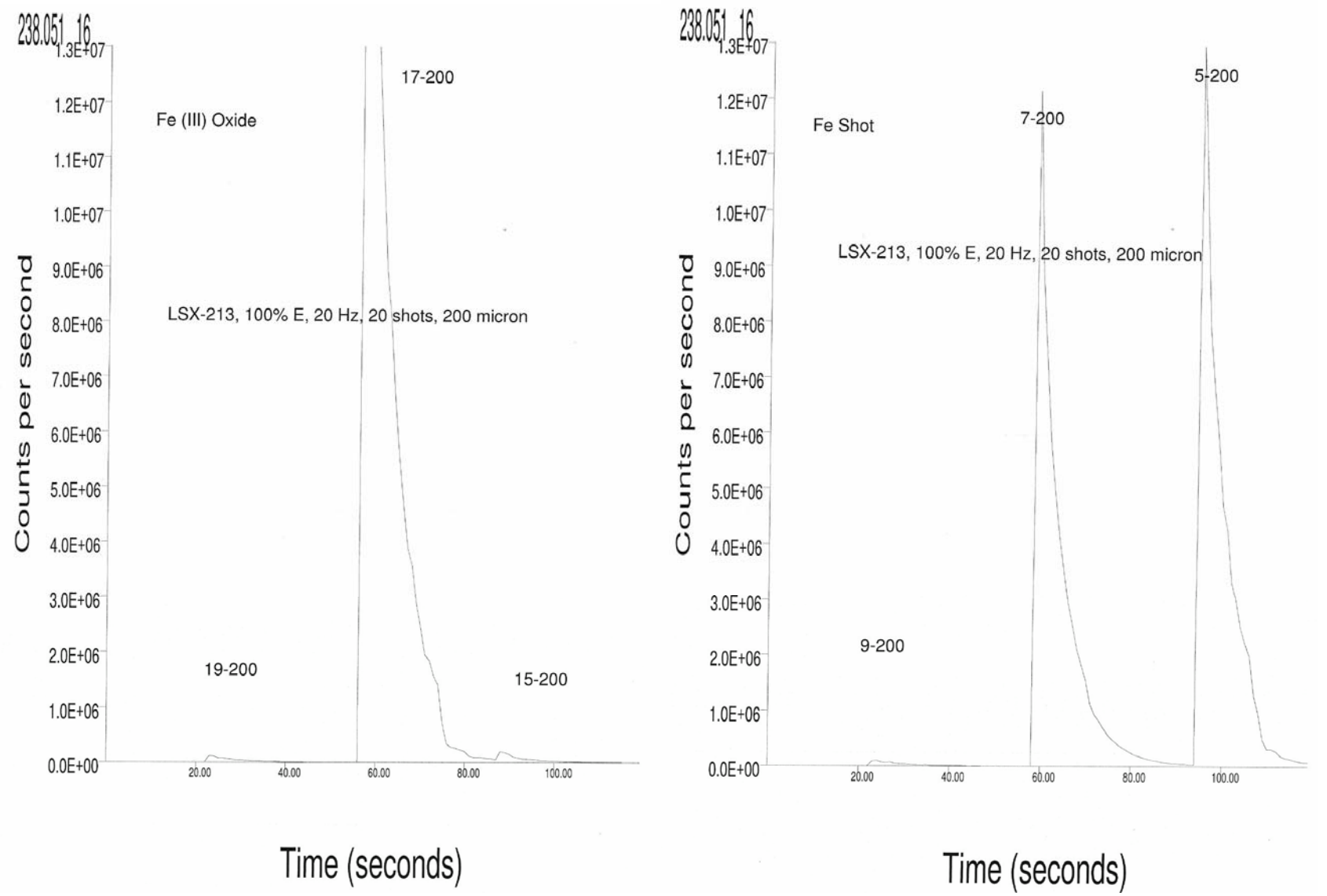

Figure 10. LA-ICP-MS signal showing the pH dependence on the affinity of U for solid Fe (III) oxide (left) and Fe shot (right) after 200 hours. Sample 9-200 and 19-200 are the blanks (without U spike); samples 7-200 and 17-200, and 5-200 and 15-200 correspond to an initial solution concentration of ~10 ppm and an initial pH of ~8.5 and 3.5, respectively. Non-Q, for informational purposes only. Source: SN-UCCSN-UNLV-086 Vol. 1.

7.2.4 Characterization of the Solids by XRD

Samples of reacted shot and Fe_2O_3 were investigated by X-Ray Diffraction (XRD) to shed light on the mineral surfaces and their sorbed species. For the Fe-shot, solid corrosion products that had sloughed off the Fe-shot were filtered and studied by XRD. There appears to be small subtle peaks mirroring the database pattern for goethite at the top of figure 11; however, overall the lack of well defined peaks is indicative of an amorphous material (Fig. 11). The spectra for the iron (III) oxide samples reflected that of the starting material.

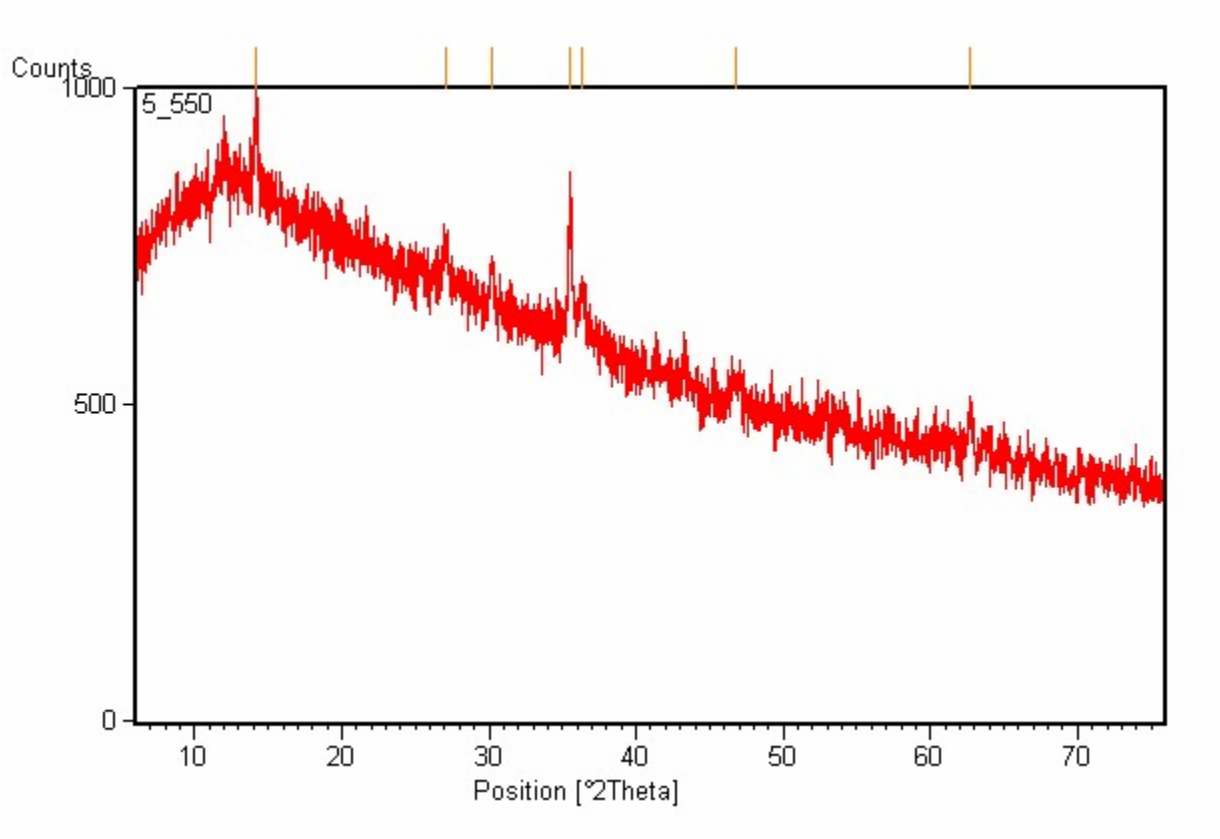

Figure 11. XRD spectra of corrosion product sloughed off Fe-shot (sample 5-550) and captured on 0.45 micron filter. Non-Q, for information purposes only. Source: SN-UCCSN-UNLV-086 Vol. 1. The XRD pattern for the database lines on the top of the figure corresponds to goethite.

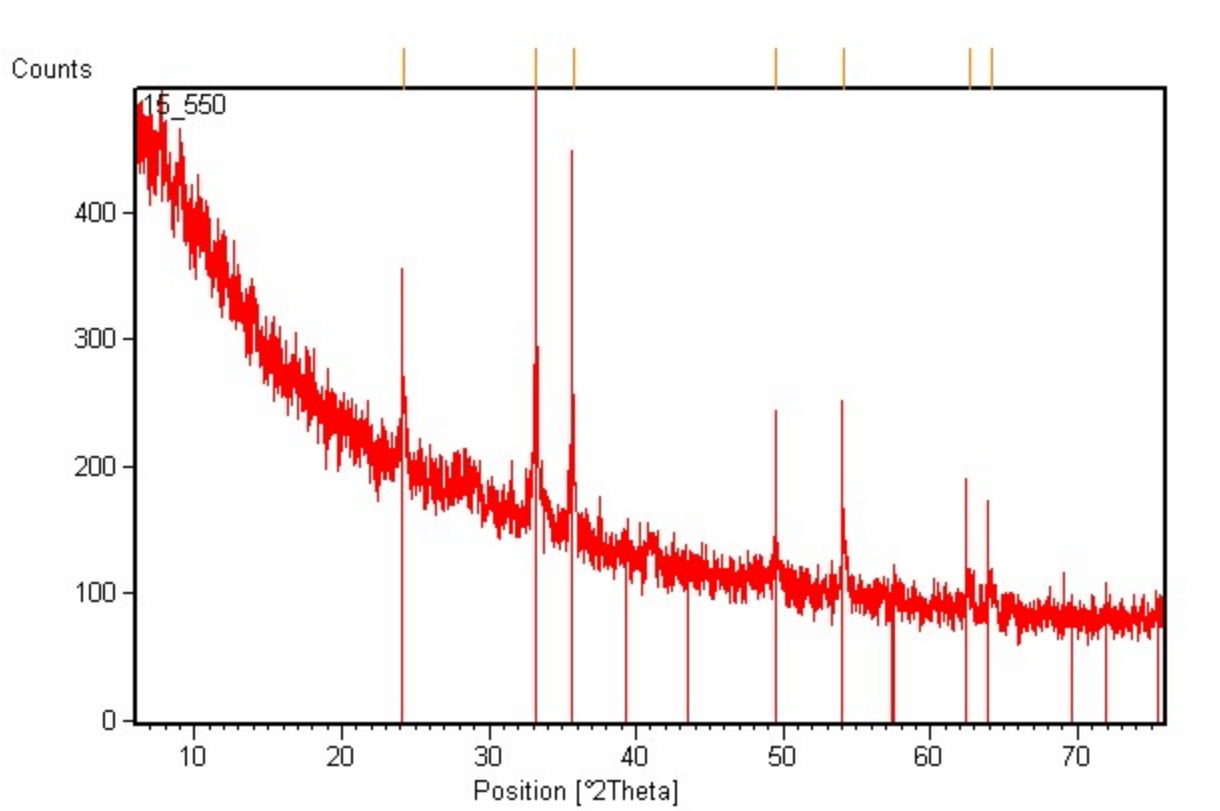

Figure 12. XRD spectra for sample 15-550 showing peaks characteristic of hematite, the starting material. No peaks for U, Gd, and Nd were observed. Non-Q, for information purposes only. Source: SN-UCCSN-UNLV-086 Vol. 1. The XRD pattern for the database lines on the top of the figure corresponds to hematite.

7.2.5 Concentrations of U on the Surface of Iron Shot and Iron (III) Oxide

Figures 13 and 14 were generated using TOF-ICP-MS so that the elemental signals were collected essentially simultaneously. Tables 4 and 5 present estimated uranium concentrations for the surface of iron shot and iron oxide after 200 hours of reaction time. Section 5.3.2 describes how these concentrations were determined. The calibration equation (y = signal intensity; x = concentration in ppb) for the Fe-shot was y = 1132.8x + 1409.1 and for Fe (III) Oxide was y = 821.6x + 16.922. The higher the peak is in the figures the higher the concentration reported in the tables. Concentrations were highest for the iron shot exposed to the 10 ppm solution. As discussed earlier, after 200 hours the pH of the iron shot solutions were similar and thus there appears to be little difference between the samples 1-4 and 5-8. However, for the iron oxide the U concentrations were low for those samples starting at low pH and relatively high for those starting at high pH. It should be noted that in most cases the sample was too small to do replicate analysis on the same iron shot or oxide particle. Also the ablation process may result in localized deposition of material skewing subsequent analysis.

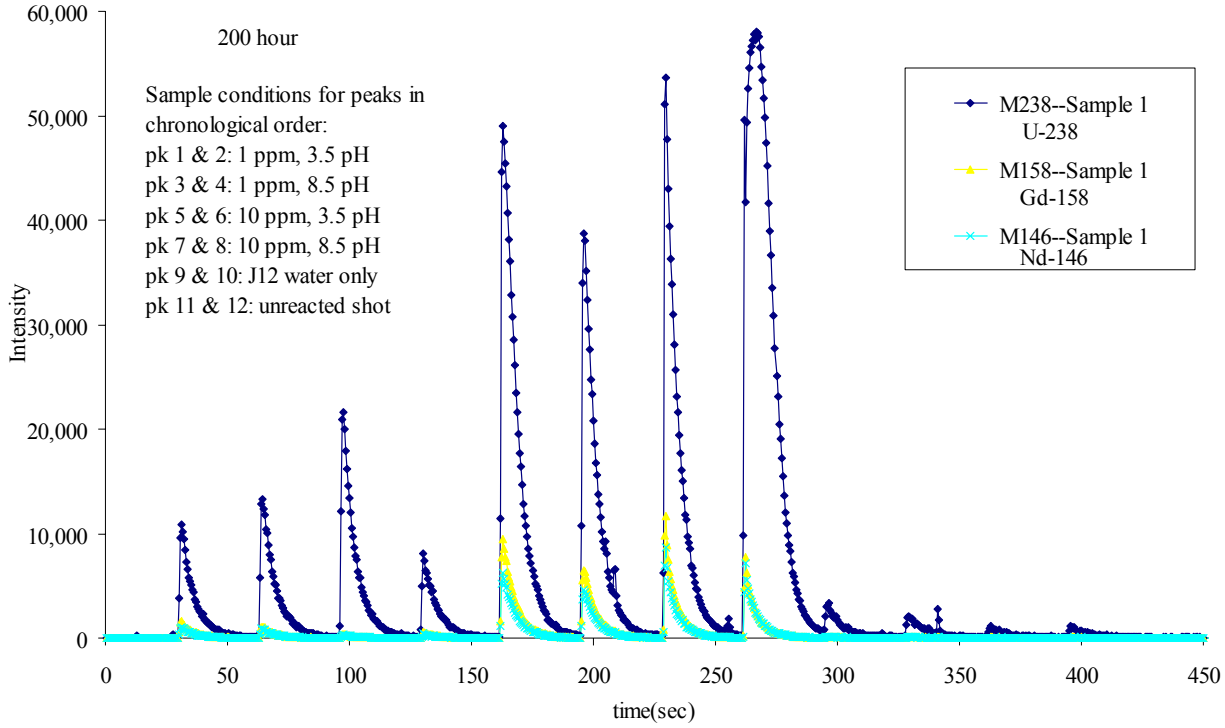

Figure 13. U, Gd, and Nd signals from the ablation of Fe-shot from various reaction mixtures after 200 hours. DTN: R03JC.003

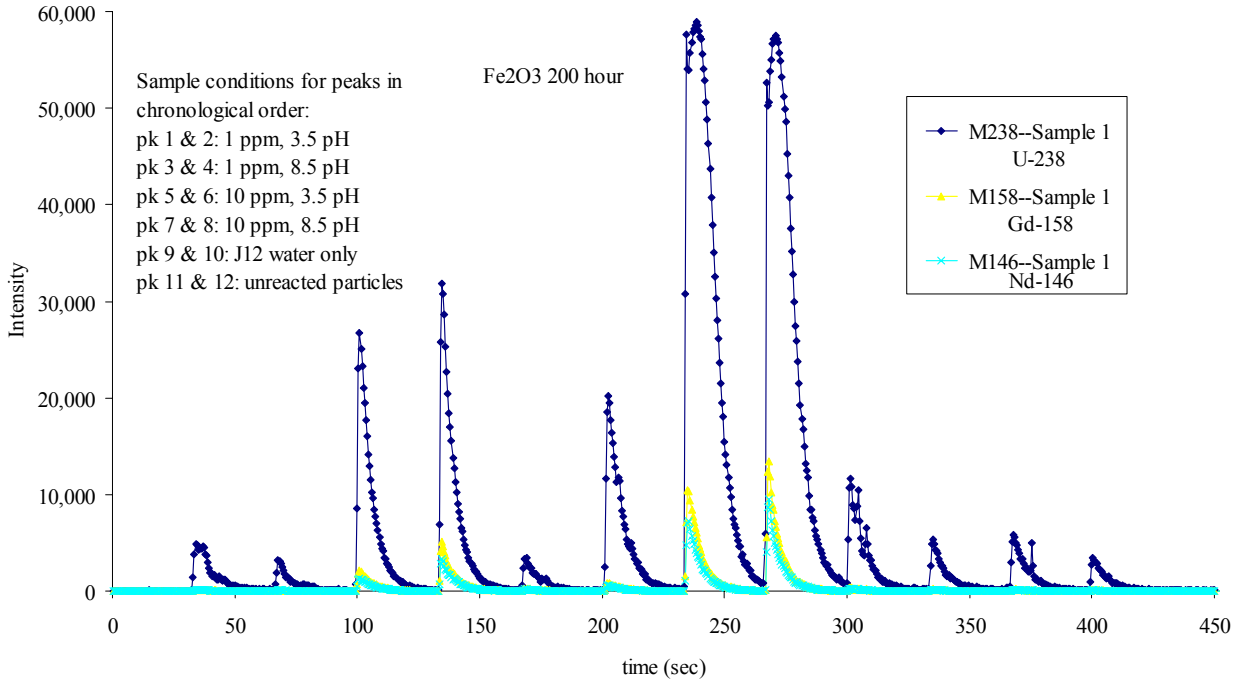

Figure 14. U, Gd, and Nd Fe signals from the ablation of Fe(III)Oxide from various reaction mixtures after 200 hours. Note: As a low pH sample, peak 6 is anomalously high. DTN: R03JC.003

Table 4. Estimated Uranium Concentrations for the Surface of Fe Shot after 200 hours

Peak #	Sample	Peak Intensity	Peak Intensity Relative % Difference (RPD)	Average Peak Intensity for Duplicates	Background subtracted Peak Intensity	Approximate Concentration (ppb)
1	pH 3.5, 1 ppm	10909	19.8	12107	11008	8.5
2		13305				
3	pH 8.5, 1 ppm	21565	91.3	14808.5	13709.5	10.9
4		8052				
5	pH 3.5, 10 ppm	49053	23.7	43862.5	42763.5	36.5
6		38672				
7	pH 8.5, 10 ppm	53591	8.0	55826	54727	47.1
8		58061				
9	J12 only	3314	48.0	2673	1574	0.1
10		2032				
11	Blank	1116	3.1	1099	NA	NA
12		1082				

The concentrations are approximate and should be viewed with caution because appropriate iron shot and iron oxide standards do not exist and because the depth and mass of the ablation crater was not determined. Note that some duplicates have relatively high RPD. Calibration was performed using NIST glass instead. Blank = unreacted shot; NA = Not Applicable. DTN: R03JC.003.

Table 5. Estimated Uranium Concentrations for the surface of Fe_2O_3 particles after 200 hours

Peak #	Sample	Peak Intensity	Peak Intensity Relative % Difference (RPD)	Average Peak Intensity for Duplicates	Background subtracted Peak Intensity	Approximate Concentration (ppb)
1	pH 3.5, 1 ppm	4848	42.5	3999	-595	<5.6
2		3150				
3	pH 8.5, 1 ppm	26678	17.5	29242	24648	30.0
4		31806				
5	pH 3.5, 10 ppm	3446	142	11821.5	7227.5	8.8
6		20197				
7	pH 8.5, 10 ppm	58986	2.5	58270.5	53676.5	65.3
8		57555				
9	J12 only	11683	74.4	8514.5	3920.5	4.8
10		5346				
11	Blank	5802	52.6	4594	NA	5.6
12		3386				

The concentrations are approximate and should be viewed with caution because appropriate iron shot and iron oxide standards do not exist and because the depth and mass of the ablation crater was not determined. Note that some duplicates have relatively high RPD. Calibration was performed using NIST glass instead. Blank = unreacted shot; NA = Not Applicable. DTN: R03JC.003.

7.3 Task ORD-RF-02 Samples

As discussed in Section 5.4, potassium bromide (KBr) pellets were transferred from Task ORD-RF-02 to this study for evaluation by LA-ICP-MS. Six of these pellets (6-20, 6-20D, 6-23, 7.5-33, 9-40, and 9-68) were randomly selected for initial analysis and method development. The Si signal is plotted in figure 15 (each peak corresponds to an ablation event). Because no Si was added to the samples, it must have been introduced from the glass sample introduction system or elsewhere. Because of the relatively high signal background, we will not discuss these data further. In contrast, Fe and U produced widely varying signal intensities with reasonable backgrounds under the same measurement conditions for different locations within the same sample pellet. Figure 16 shows the lack of reproducibility for seven ablation events for Fe and U, respectively. Figure 17 shows the poor reproducibility for U for a different sample. The intent at this juncture was to look at reproducibility of the signal not to quantify the signal, therefore no calibration curve was generated. Consequently, detection limits were not determined.

The number of laser firings (shots) used for this analysis was determined by the level of signal generated. For Si a single shot yielded sufficient signal above instrumental background, whereas Fe and U employed 200 and 100 shots, respectively. Each of these bursts was then applied to different areas on the surface of the pellet and the elemental signal monitored. The purpose of this analysis was not to quantify the elements but to gauge the reproducibility with respect to LA.

Overall, there appears to be a lack of homogeneity at the 200 micron level for U and Fe. While this may have no impact on the spectrometry study that essentially uses the entire pellet, it renders microanalysis by LA-ICP-MS difficult and quantitative measurements meaningless with the laser ablation conditions used. In some cases, the poor homogeneity can be seen visually on the pellet with the LA camera through color changes and spotted regions. It is possible that variability in thickness of the pellet is also impacting ablation properties. In any case, given the poor reproducibility quantitative measurements and analysis of more samples were not conducted. Further method development, such as scanning a larger region and subsequently integrating the entire signal, may have helped but instrumental problems and time constraints would not allow this work.

Qualitatively, however, a pattern was observed. U and Fe were seemingly inversely correlated. A single shot was fired into six different pellets and the U and Fe signals monitored. The U variability between samples is shown in figures 6 and 7; the Fe variability between samples in figures 8 and 9. Comparing the patterns between these two sets of spectra, one can see that they are generally opposite in trend (despite internal variability). The correlation (r) was 0.217 for U versus Fe for one set of data using peak areas (Fig. 18 left vs. Fig 17 right) and 0.636 for the other set (Fig 18 right vs. fig 17 left).

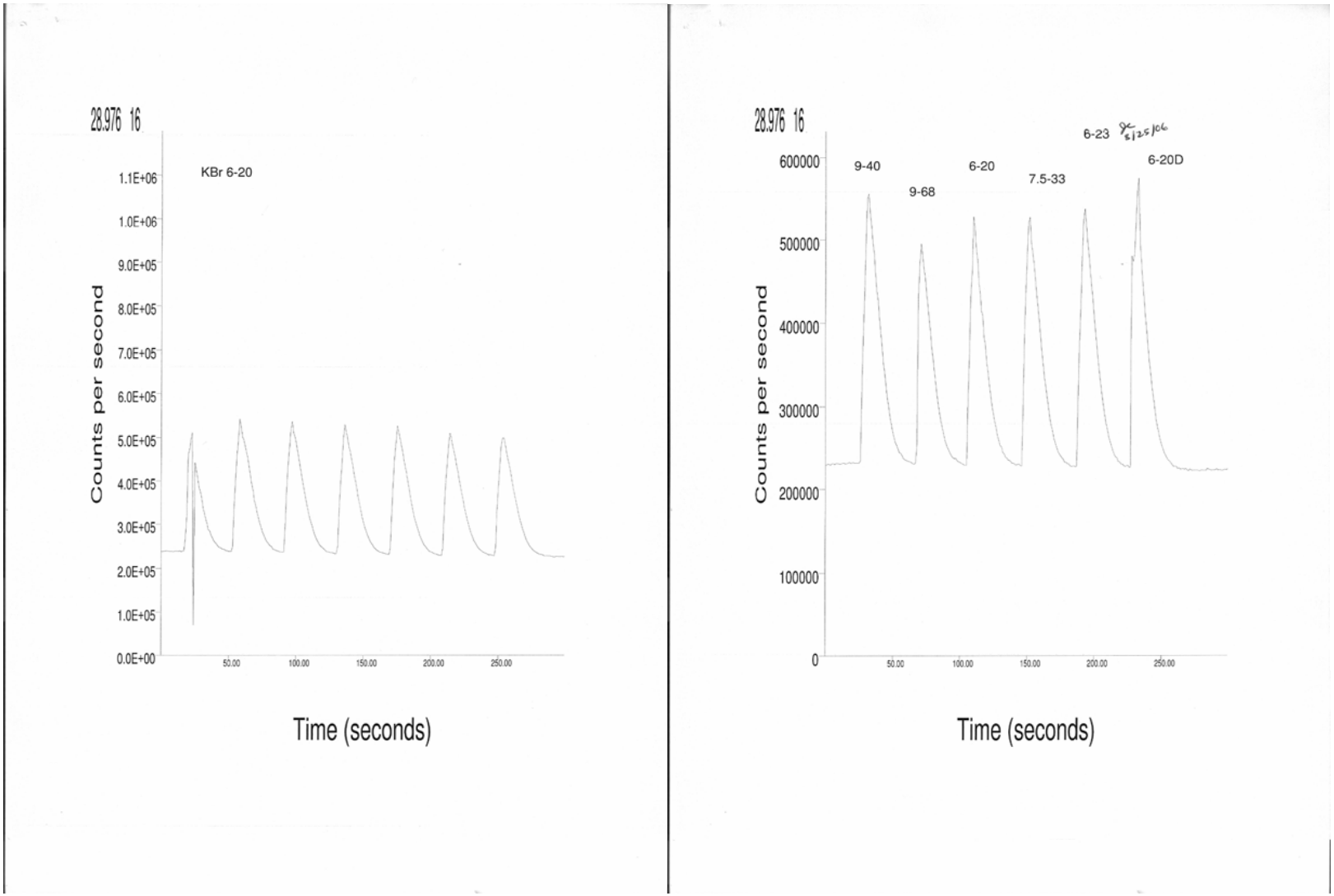

Figure 15. ICP-MS Si signal within (left) and among (right) samples. It is possible that the high baseline may be improved using an all Teflon sample introduction system. Non-Q, for informational purposes only. Source: SN-UCCSN-UNLV-086 Vol. 1

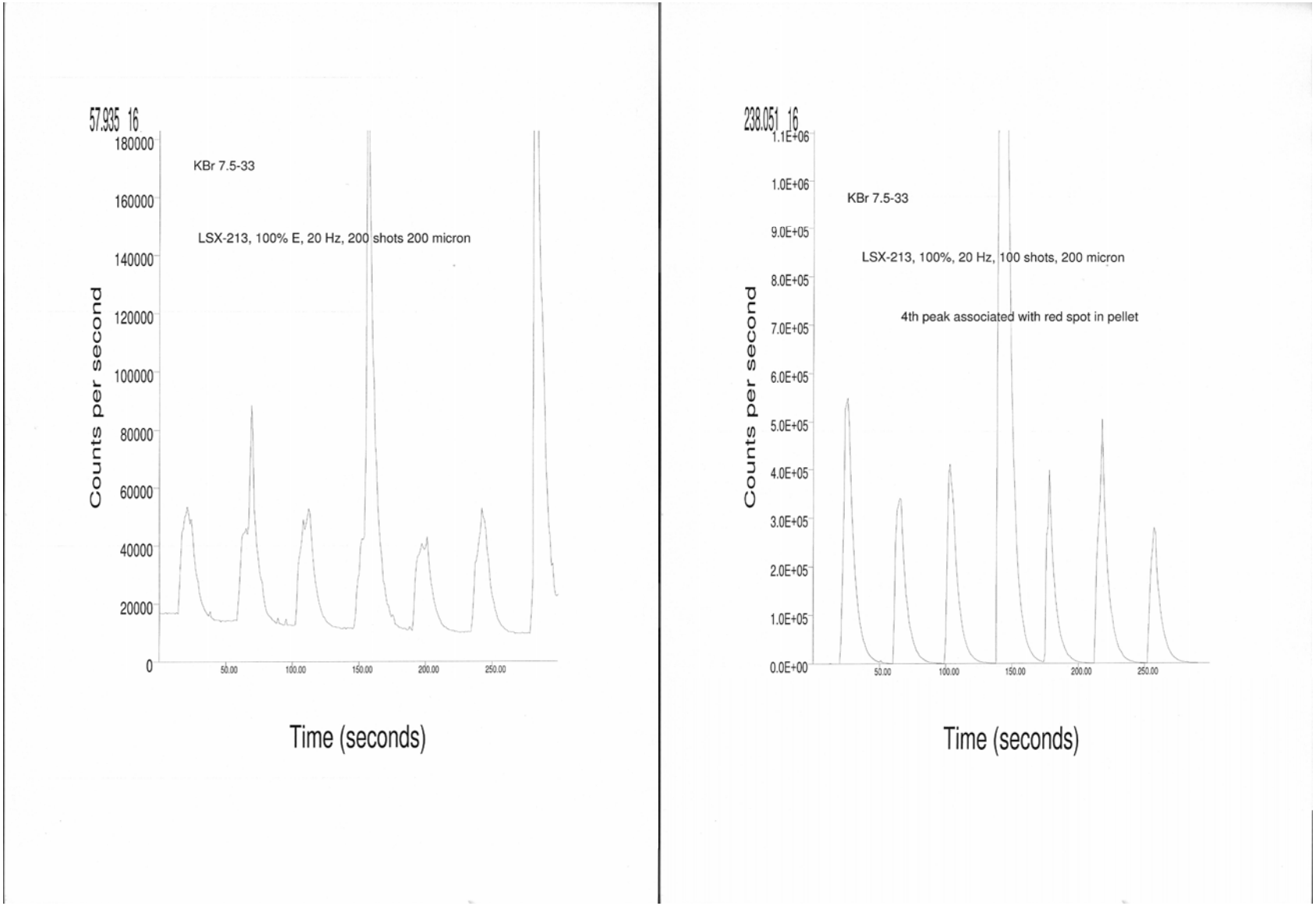

Figure 16. ICP-MS signal showing poor reproducibility for Fe (left) and U (right) within a sample. The laser was fired under the same conditions at different locations on the same KBr pellet. Non-Q, for informational purposes only. Source: SN-UCCSN-UNLV-086 Vol. 1.

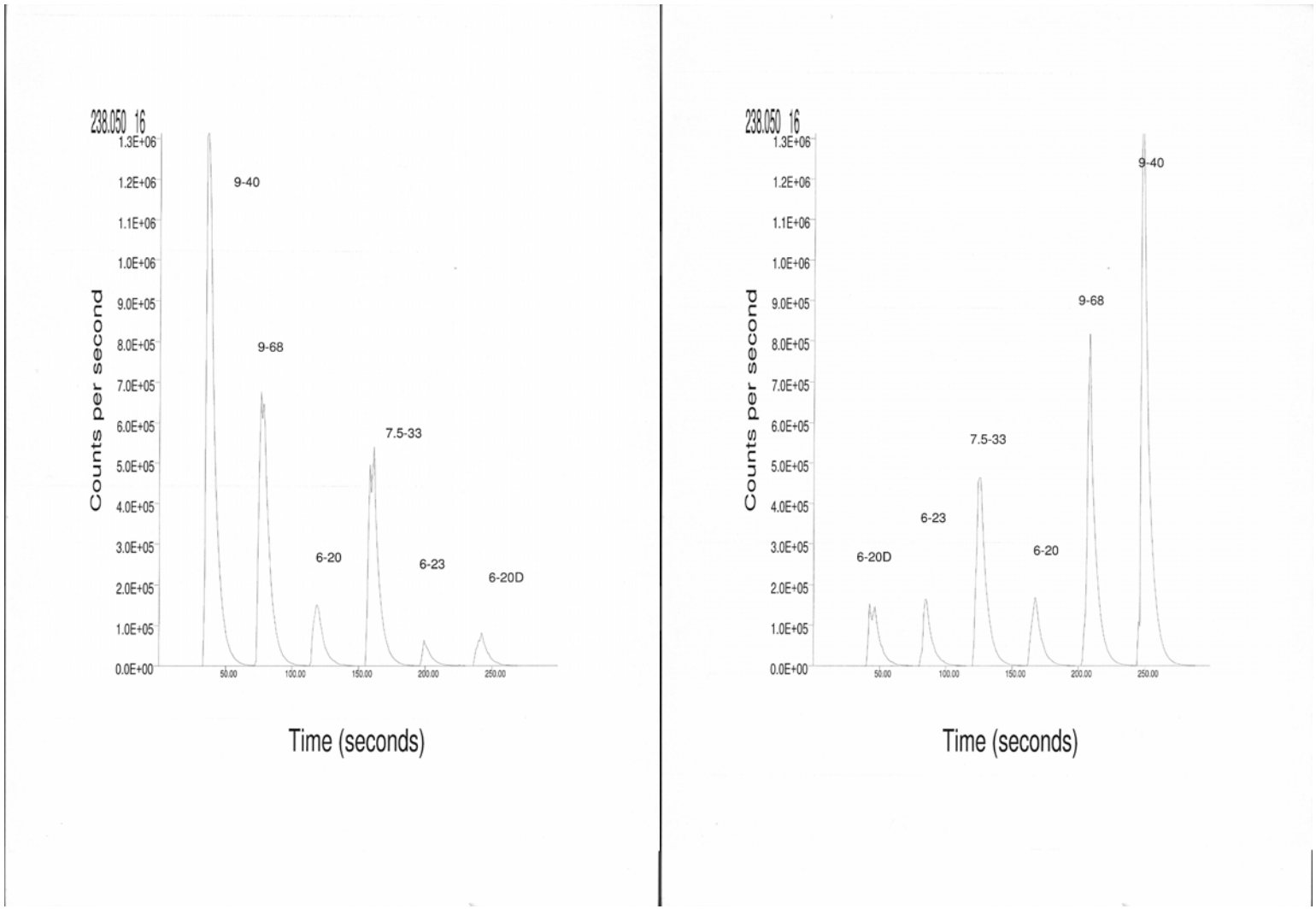

Figure 17. ICP-MS U signal showing variability among samples. The samples were analyzed in reverse order (right side) but generally show the opposite pattern despite internal variability. Non-Q, for informational purposes only. Source: SN-UCCSN-UNLV-086 Vol. 1.

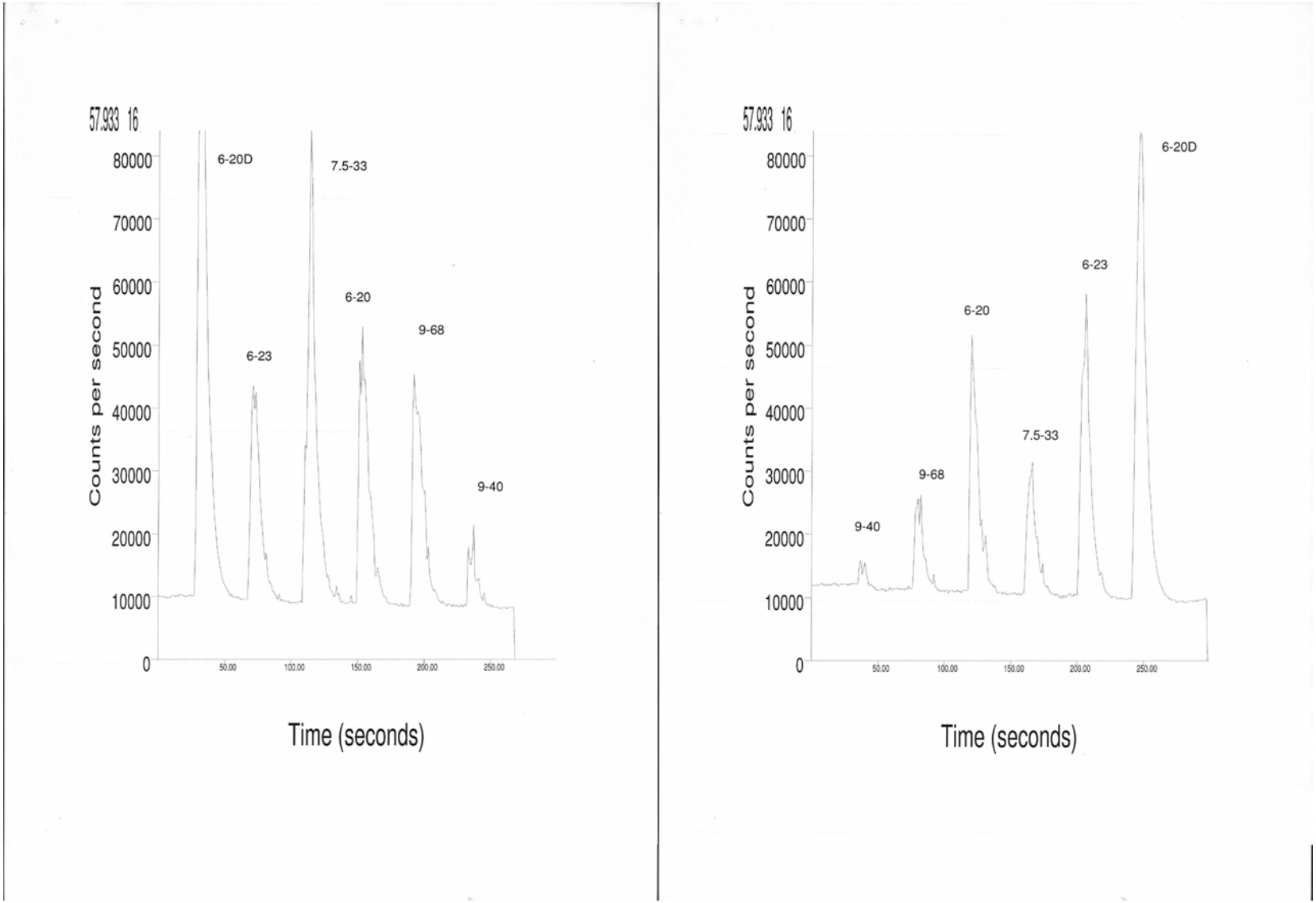

Figure 18. ICP-MS Fe signal showing variability among samples. The samples were analyzed in reverse order (right side) and generally show the opposite pattern. The pattern appears opposite to that of U in Fig. 17. Non-Q, for informational purposes only. Source: SN-UCCSN-UNLV-086 Vol. 1.

7.4 Conclusions and Recommendations based only on Q Data

- pH plays an important role in the behavior of U with corrosion products. Aqueous solutions reacting with iron shot generally showed a steady and significant increase in pH over 200 hours, with one increasing from a ~3 to ~10. For iron (III) oxide, there was no change in pH for the low pH (~3) solution and a slight increase for the high pH (~8) solutions

- A QA-approved method was developed for the semi-quantitative determination of elements in solids using laser ablation inductively coupled plasma mass spectrometry (LA-ICP-MS). The method is published as an implementing procedure on the NSHE QA Program's website (http://hrc.nevada.edu/QA/).

- LA-ICP-MS has proved useful in the direct analysis and study of corrosion products for U. It offers micro-analysis capabilities down to ~50 micron resolution (crater diameter) based on the matrices examined in this work.

- The LA-ICP-MS system and expertise acquired during the project is available to DOE to meet its future research needs. It is recommended that it be considered as a possible screening tool to identify those samples with sufficient analyte distribution before submitting samples that may require more costly surface characterization.

- Sample morphology can vary within a material. If it is possible to identify and target phases, the relative concentration of each phase can be evaluated. In this study no attempts were made to apply the methodology to specific phases in samples or standards. Future work can benefit from this type of investigation.

- A complete mass balance of the U, Gd, Nd, Fe-shot system was unattainable in part because sample surface areas and mass transport during ablation were not determined and because of variability in the concentrations determined by LA-ICP-MS. Mass balance information is important for evaluating the technique particularly when determining the total concentration of metal ion sorbed to the solid phase. Future work should include experimental design and measurements that will allow a mass balance so that the method can be validated by this mass balance approach.

7.5 Summary of Corroboration Including UQ Data

- Iron chips corroded in the presence of aqueous uranium yielded an irregular shaped and colored surface. For this material it was found that a single laser ablation shot at 100% energy (E), 1 Hz, and 50 μm spot was sufficient to produce a large repetitive signal for U using the TOF ICP-MS.

- Ablation of the lighter whitish areas of the corroded chip produced the highest Fe-normalized U signals. Scanning electron microscope measurements corroborated that the lighter regions contained the highest U concentrations, suggesting LA-ICP-MS may be useful as a screening technique to identify samples for further characterization by more costly techniques.

- LA-ICP-MS signals for U and Gd increased on the surface of iron shot as a function of reaction time for the solution with a low starting pH.

- Uranium and Gd remained in solution and were minimally sorbed to iron (III) oxide at low pH (~3), whereas at "high" pH (~8) the elements are incorporated onto the surface of the oxide.

- XRD analysis of solid corrosion products that had sloughed off the Fe-shot were consistent with an amorphous oxide. The spectra for the iron (III) oxide samples reflected that of the starting material.

- Pressed KBr pellets obtained from Task ORD-RF-02 lacked homogeneity at about the 200 micron level for U and Fe, based on the results from single laser ablation shots over ~7 locations on the surface of the pellet. Thus, LA-ICP-MS may not be suitable for analysis of potassium bromide (KBr) pellets formed from pressing of solids due to these homogeneity issues based on the ablation parameters used in this study

- Repetitive ablation of iron shot at the same location suggests surface layers of U and Gd increase with reaction time.

8.0 INPUTS AND REFERENCES

8.1 Inputs

Figure	Data ID Number (DID) or Source of Information
1	NA/UQ
2	SN-UCCSN-UNLV-086 Vol. 1; UQ
3	SN-UCCSN-UNLV-086 Vol. 1; UQ
4	NA/UQ
5	NA/UQ
6	R03JC.002
7	SN-UCCSN-UNLV-086 Vol. 1; UQ
8	SN-UCCSN-UNLV-086 Vol. 1; UQ
9	R03JC.001
10	SN-UCCSN-UNLV-086 Vol. 1; UQ
11	SN-UCCSN-UNLV-086 Vol. 1; UQ
12	SN-UCCSN-UNLV-086 Vol. 1; UQ
13	R03JC.003
14	R03JC.003
15	SN-UCCSN-UNLV-086 Vol. 1; UQ
16	SN-UCCSN-UNLV-086 Vol. 1; UQ
17	SN-UCCSN-UNLV-086 Vol. 1; UQ
18	SN-UCCSN-UNLV-086 Vol. 1; UQ
Table	
1	R03JC.003
2	NA/UQ
3	SN-UCCSN-UNLV-086 Vol. 1; UQ
4	R03JC.003
5	R03JC.003
NA = Not Applicable; UQ, for informational purposes only	

8.2 Cited References

Barner, J.O. (1985) Pacific Northwest Laboratoy Report PNL-5109.

Becker J.S., Pickhardt C., Dietze, H.J. (2000) *International J. of Mass Spectrom*. 202, 283-297.

Becker J.S., (2002) *J. Anal. At. Spectrom*. 17, 1172-1185.

Becker J.S., Dietze H.J. (2004) *Frsenius' J. Anal. Chem.* 368: 23-30.

Devos W. Senn-Luder M., Moor C., Salter C. (2000) *Fresenius' J. Anal. Chem.* 366: 873-880

Dodge C. J., A.J. Francis, J.B. Gillow, G.H. Halada, C. Eng and C.R. Clayton (2002) "Association of Uranium with Iron Oxide Typically Formed on Corroding Steel Surfaces" *Environ. Sci. and Tech*. 36(16), 3504-3511.

Duff M.C., Coughlin J.U., Hunter D.B.(2002) "Uranium co-precipitation with iron oxide minerals" *Geochimica et Cosmochimica Acta*, Vol. 66, No. 20, 3533–3547.

Gunther D., Hattendorf B., Latkoczy C. (2003) "Laser ablation ICPMS" *Anal. Chem*. Aug. 341A-347A.

Hull, L.; Pace, M.; Leasing, P.; Rogers, R.; Mizia, R.; Propp, A.; Shaber, E.; and Taylor, L. 2000. *Advanced Neutron Absorbers for DOE SNF Standardized Canister-Feasibility Study.* DOE/SNF/REP-057, Rev. 0. Idaho Falls, Idaho: U.S. Department of Energy, Idaho Operations Office. ACC: MOL.20051021.0173

Hyeon L.J., Byrne R.H. (1994) *Geochim. Et Cosmochim. Acta* 58:4009-4016.

Johannesson K.H., Zhou X., Guo C., Stetzenbach K.J., Hodge V.F. (2000) "Origin of rare earth element signatures in groundwaters of circumneutral pH from southern Nevada and eastern California, USA" *Chemical Geology* 164, 239-257.

Kim C.W., Wronkiewicz D.J., Finch R.J., Buck E.C. (2006) "Incorporation of Cerium and Neodymium in uranyl phases, *J. of Nucl. Materials* 353, 147-157.

Leloup C., Marty P., Dall'ava D. Perdereau M. (1997) *J. Anal. Atom. Spec.* 12: 945-950.

Moyes L.N., Parkman R.H., Charnock J.M., Vaughan D.J., Livens F.R., Hughes C.R., Braithwaite A. (2000) "Uranium uptake from aqueous solution by interaction with goethite, lepidocrocite, muscovite, and mackinawite: An X-ray absorption spectroscopy study", Environ. Sci. and Tech. 34, 1062-1068.

Pabalan R.T., Turner D.R., Bertetti F.P. (1998) "Uranium sorption onto selected mineral surfaces: key geochemical parameters" in Adsorption of Metals by Geomedia: Variables, Mechanisms and Model Applications. Edited by Everett A. Jenne. Academic Press.

Pickhardt, C., Brenner, I., Becker, J.S, Dietze, H.J. (2000) *Fresenius J. Anal. Chem*. 1, 368.

Radulescu H., Moscalu D., Montierth L. (2000) *Proc. Of Spectrum 2000: Int. Conference on Nuclear and Hazardous Waste Management,* American Nuclear Society, La Grange park, Ill.

Seltzer MD. (2003) *Appl Spectrosc* 57:1173-1177.

Shannon R.D. (1976) Acta Cryst. A32, 751.

Strnad L, Mihaljevic M. (2005) *Mineralogy and Petrolgoy* 84:47-68.

Vors E., Semerok A, Wagner J.F. (1999) *Applied Physics A: Materials Science and Processing*, 69: S165-S166.

Weis P., Beck H.P., Gunther D. (2004) *Anal. Bioanal. Chem.* 212-224.

Wood SA. 1990. The aqueous geochemistry of the rare-earth elements and Yttrium. 1. Review of available low-temperature data for inorganic complexes and the inorganic REE speciation of natural waters. Chem Geol. 82:159–186.

Wronkiewicz D.J., Bates J.K., Wolf S.F., Buck E.C. (1996) *J. Nuc. Mater*. 238, 78.

Wronkiewicz D.J., Bates J.K., Gerding T.J.. Veleckis, E., Tani B.. (1992) *J. Nuc. Mater*.190, 107.

9.0 SOFTWARE

Not applicable.

10.0 ATTACHMENTS

Not applicable.